NATIONAL ADVISORY COMMITTEE FOR AERONAUTICS

TECHNICAL NOTE 4382

INVESTIGATION OF BOILING BURNOUT AND FLOW STABILITY FOR WATER FLOWING IN TUBES

By Warren H. Lowdermilk, Chester D. Lanzo, and Byron L. Siegel

Lewis Flight Propulsion Laboratory
Cleveland, Ohio

Washington

September 1958

NATIONAL ADVISORY COMMITTEE FOR AERONAUTICS

TECHNICAL NOTE 4382

INVESTIGATION OF BOILING BURNOUT AND FLOW STABILITY FOR WATER FLOWING IN TUBES

By Warren H. Lowdermilk, Chester D. Lanzo, and
Byron L. Siegel

SUMMARY

Boiling-burnout heat-transfer rates were measured with water flowing vertically upward in electrically heated tubes. Flow stability in the experimental test section during burnout was affected by the amount of pressure drop across a throttling valve located upstream. As the restriction pressure drop across the valve was increased, the magnitude of the flow fluctuations in the test section decreased and the burnout heat flux increased until the pressure drop exceeded a critical value. For further increases in pressure drop, the flow was steady and the burnout flux was independent of the pressure drop across the throttling valve. The minimum restriction values required to stabilize the flow varied nearly linearly from 5 to 100 pounds per square inch with an increase in velocity from 0.5 to 40 feet per second; these values were independent of the pressure drop across the test section.

A compressible volume introduced in the flow system between the throttling valve and the test section resulted in unsteady flow during burnout. The larger the volume, the greater were the flow fluctuations and the lower were the attendant burnout heat-transfer rates.

Burnout heat-transfer rates were measured in the stable-flow region for a range of velocity from 0.1 to 98 feet per second, pressure ranging from atmospheric to 100 pounds per square inch, inlet subcooling from 0° to 140° F, tube diameters from 0.051 to 0.188 inch, and length-to-diameter ratios from 25 to 250. The resulting burnout heat fluxes ranged from 0.9 to 13.2×10^6 Btu per hour per square foot. Net steam was generated for all stable-flow conditions, and two regimes of burnout were obtained. In the low-velocity high-exit-quality region, the data were correlated by the relation $(Q/S)\ D^{0.2}\ (L/D)^{0.85} = 270\ G^{0.85}$ for $G/(L/D)^2 < 150$, and in the high-velocity low-exit-quality region by $(Q/S)\ D^{0.2}\ (L/D)^{0.15} = 1400\ G^{0.5}$ for $G/(L/D)^2 > 150$, where Q/S

is the heat flux, D is the inside tube diameter, L/D is the length-to-diameter ratio, and G is the mass-flow rate. At the transitional value of $G/(L/D)^2$ of 150, the exit quality varied from 40 to 60 percent.

INTRODUCTION

The high heat-transfer rates obtainable with the forced-convection nucleate boiling process are attractive for use in cooling components of rocket motors and nuclear reactors. For most applications, a knowledge of the maximum heat-transfer rate, or boiling burnout, is required. Many studies of boiling burnout have been made with a variety of coolants and coolant-flow systems. Empirical correlations, while successfully correlating results from a single study, have not met with much success when used to compare results of other investigations. This variation has resulted in much uncertainty in predicting maximum heat-transfer rates and is due largely to the effects of flow-system characteristics on flow instability and boiling burnout.

Relations between flow instability and boiling burnout are presented in reference 1. Reference 2 shows that, in a flow system using a centrifugal pump, flow stability and burnout were affected by the pump characteristics. In reference 3, a pressure-volume coolant supply was used. It was found (ref. 3) that flow instability and burnout occurred at low heat fluxes when the flow rate was controlled by a restriction located downstream of the experimental test section, and that a tenfold increase in burnout heat flux was obtained by greatly restricting the flow upstream of the test section and discharging the flow from the test section either into a compressible-volume tank or to the atmosphere.

These results indicate that the flow-system characteristics have a large-order effect on flow stability and the attendant burnout heat fluxes. Hence, the factors affecting flow stability need to be defined in order to compare the burnout results obtained by various investigators using a variety of flow systems.

The purpose of the present study is to investigate the effects of flow-system characteristics on flow stability and burnout. An open cycle or once-through flow system similar to that used in reference 3 was chosen, and the flow was restricted upstream of the test section and discharged into a compressible volume at the exit of the test section. With this system, flow stability and burnout can be defined by determining the pressure drop across the flow restriction in addition to usual burnout variables, such as flow rate, pressure, temperature, and tube geometry.

The effects of flow restriction and compressible volume on flow stability are surveyed with water flowing in tubes. In the stable-flow region, burnout is determined for a wide range of tube geometry and flow-rate values. The results are presented in graphical and tabular form.

SYMBOLS

The following symbols are used in this paper:

D	inside tube diameter, ft
E	voltage drop across test section, v
G	mass-flow rate, lb/(hr)(sq ft)
h_f	enthalpy of saturated liquid, Btu/lb
$h_{f,g}$	latent heat of vaporization for pressure at exit of test section, Btu/lb
h_1	enthalpy at test-section inlet, Btu/lb
I	current flow through test section, amp
K	conversion factor, watts to Btu/hr
L	length of test section between inner faces of electrical bus clamps, ft
L/D	length-diameter ratio, dimensionless
p	pressure, lb/sq in.
Q	total heat input to test section, Btu/hr
Q/S	heat flux, Btu/(hr)(sq ft)
S	inside surface area of tube, sq ft
T	temperature, ^{o}F
W	flow rate, lb/hr
x	exit quality of steam

APPARATUS

Arrangement of Apparatus

Preliminary. - Schematic diagrams of the arrangements of the apparatus are shown in figure 1. The original arrangement shown in figure 1(a) is similar to arrangement B used in reference 3. The distilled-water supply system included two 10-gallon storage and degassing tanks and two 5-gallon accumulators. Degassed water was contained in the neoprene bladders in the accumulators. Nitrogen, supplied to the outside of the accumulator bladders through a pressure-regulating valve, was used to force the water from the accumulators through the flow-control valve, flowmeters, preheater, and test section into the discharge tank.

Power was supplied to the preheater from a 10-volt, 1000-ampere, alternating-current supply. The preheater consisted of a 3-foot length of 3/8-inch-diameter stainless-steel tubing.

Electric power was supplied to the test section from a 208-volt, 60-cycle supply line through an autotransformer and a 16:1-ratio power transformer. The maximum power available at the test section was 25 volts at 2500 amperes.

The flow-system piping upstream of the test section consisted of 3/8-inch-diameter stainless-steel tubing with 1/16-inch-thick walls. A 1-inch-diameter hose was used to connect the exit end of the test section to the discharge tank in order to minimize flow restrictions downstream of the point of burnout.

Final. - The final arrangement of the apparatus is shown in figure 1(b). The accumulators were connected in series instead of parallel in order to eliminate the diffusion of nitrogen into the water flowing through the test section. The test section and preheater were combined into a single tube. The throttling and flow-control valves were relocated just upstream of the test section and preheater; two valves were used to provide both coarse and vernier control of the flow rate.

Experimental Test Section

Diagrams of the test section are shown in figure 2. A typical section, shown in figure 2(a), was made from type-347 stainless-steel tubing. In all the test sections except the 0.188-inch-diameter tubes, a stainless-steel bushing was silver-soldered to each end of the section, and then a collar (3/8-in. diam., 5/8-in. long) was placed over the bushing and was silver-soldered to the bushing. The heated length was the distance between the inner faces of the collars. The unheated

length at each end of the test section was 3/16 inch, compared with the 7/8-inch length used in reference 3. The test-section dimensions were as follows:

Inside diameter, in.	Heated length-diameter ratio	Unheated length-diameter ratio	Wall thickness, in.	Wall thickness-inside diameter ratio
0.051	50,100,150,200,250	7.3	0.033	0.65
.051	250	7.3	.074	1.45
.076	50,100,150,200,250	4.9	.040	.53
.096	50,100,150,200,250	3.9	.057	.59
.123	25,50,100,150,200,250	3.0	.065	.53
.156	25,50,100,150,200,250	2.4	.048	.31
.188	25,50,100,150,200,250	2.0	.0935	.50

The test sections were polished and degreased prior to installation in the system. Each newly installed section was degreased by preheating to about 700° F for 5 to 10 minutes before the tube was filled with water.

For the majority of the runs conducted, the heated length of the test section was varied by using the 250 L/D (length-diameter) sections and clamping the inlet electric-power-supply cable at the desired location along the tube length, as shown in figure 2(b). The test section was connected to the flow system by means of 3/8-inch Ermetto fittings.

In preheated runs, the preheater power-supply cables were connected across the length of the tube that was not being heated by the main power supply.

Instrumentation

Flow rate. - Rotameters with overlapping ranges from 1 to 500 pounds per hour were used to meter the flow rate for the majority of the runs. A recording turbine-type flowmeter with a range of 50 to 400 pounds per hour was available near the conclusion of the investigation for conducting runs in which the pressure drop across the flow-control valve and test section exceeded 300 pounds per square inch. The measuring accuracy of the flowmeters is ±2 percent. The meters were calibrated after each series of runs, and daily checks were conducted.

Pressure. - Pressure upstream of the throttling and flow-control valve and in the discharge tank was measured to within a ±2 percent accuracy with Bourdon gages. A Statham pressure pickup was used to record the pressure at the inlet of the test section during the preliminary tests conducted with the apparatus arranged as shown in figure 1(a).

Temperature. - Water temperatures at the test-section inlet and exit were measured with iron-constantan thermocouples enclosed in 1/16-inch-diameter tubing located in the Ermetto fittings, as shown in figure 2(b). Mixing baffles were not used, in order to avoid flow restrictions and their effects on flow stability. The inlet water temperature was at ambient conditions for all the tests, so that mixing baffles were not required. Baffles at the exit are needed to measure the bulk temperature when subcooled burnout is encountered; but, for the range of variables investigated in the present report, net steam was generated for all the runs except in a few cases where unsteady flow was encountered, and the data were not recorded for these cases. The temperatures were measured within $\pm 1/2^{\circ}$ F.

The outside wall temperature of the test section near the point of burnout was measured with a bare, butt-welded, iron-constantan thermocouple looped around the test section 1/4 inch upstream from the exit collar of the test section (see fig. 2(b)) and held in tension against the wall with a spring. The temperature was recorded on a strip-chart recorder.

Some preliminary runs were made with thermocouples spot-welded to the test section at frequent intervals to determine wall-temperature distribution near the point of burnout. At burnout conditions the wall temperatures over the last 8 to 10 tube diameters in length of the test section fluctuated from $\pm 10^{\circ}$ to 25° F with the greatest fluctuations occurring 2 to 4 tube diameters from the exit. Accordingly, a distance of 1/4 inch from the exit of the test section was used to detect the first signs of the change in the boiling mechanism from nucleate to transitional or film boiling.

Power input. - Electric-power input to the test section and preheater was recorded on voltmeter and ammeter recorders. The recorders were calibrated, and the measuring accuracy was within ±2 percent.

EXPERIMENTAL TEST PROCEDURE

The water in the storage tanks was degassed by lowering the pressure to the value for saturation conditions at room temperature and allowing the water to boil for 15 to 20 minutes. The accumulators were

then charged with the degassed water, and the nitrogen pressure was regulated at a value of approximately 300 pounds per square inch, which was the pressure limit for the largest rotameter.

The flow rate was set at the desired value by adjusting the throttling valve and the pressure in the discharge tank. The recording instruments were put into operation, and electric power was supplied to the test section in small increments until the wall temperature started to increase rapidly. The power was then reduced slightly, and burnout was reapproached more gradually. This operation was repeated, when necessary, until the same conditions at burnout were obtained for two consecutive trials. The conditions prevailing in the tube just prior to the wall-temperature excursion were taken to be the burnout conditions. These conditions indicate the change in boiling from the nucleate to the transitional or partial-film-boiling regime. This heat flux is usually defined as the maximum or critical heat flux, rather than the burnout heat flux.

For the runs conducted at mass-flow rates greater than 2.5×10^6 pounds per hour per square foot in the test sections having a 0.051-inch inside diameter and a 0.074-inch wall thickness, the outside wall temperature exceeded 700° F, and the iron-constantan thermocouple could not be used to detect burnout. In this case, the power was increased until a visible localized hot spot occurred at the exit of the tube, which corresponds to the inception point of film boiling. The difference in heat flux between the two definitions of burnout is within the accuracy of the measurements.

METHOD OF CALCULATION

Heat Flux

The maximum or burnout heat-transfer rate was determined from the ratio of the total heat input to the test section to the inside surface area of the test section by the relation

$$\frac{Q}{S} = \frac{KEI}{\pi DL}$$

Preliminary tests showed that the wall temperature was nearly constant along the length of the test section, so the difference between the average value of heat flux and the local value at the point of burnout was assumed negligible.

Quality

The quality at the exit of the test section is defined as the weight fraction of vapor per pound of liquid-vapor mixture. This quality is based on the total electrical heat input to the test section, assuming no heat losses, by the relation

$$x = \frac{h_l + (KEI/W) - h_f}{h_{f,g}}$$

RESULTS AND DISCUSSION

Effects of System Characteristics on Flow Stability and Burnout

Nitrogen diffusion and arrangement of apparatus. - The variation of burnout heat flux with mass flow is shown in figure 3 for various arrangements of the apparatus. The results obtained with the preliminary arrangement are shown in figure 3(a). The runs were made with the discharge tank vented to the atmosphere. A pressure of 300 pounds per square inch, which was the maximum allowable pressure for the rotameters, was maintained in the accumulator, and the flow rate was controlled by the throttling valve located upstream of the rotameters.

The recordings of the pressure at the inlet of the test section indicated large pressure fluctuations at burnout, although no flow-rate variations were indicated by the rotameters. Check runs were made, and burnout heat fluxes decreased with time. A sight glass was installed at the exit of the test section at the highest elevation point in the flow system and was partially filled with water. With the flow-control valve closed and a back pressure of 100 pounds per square inch applied to the system, the water level was displaced 10 cubic centimeters; this indicated a compressible volume in the system downstream of the flow-control valve. Nitrogen bubbles were noticed occasionally in the rotameters and probably were entrapped near the exit of the rotameters, which was the highest elevation in the flow system.

The flow-control or restricting valves were relocated as near the inlet of the test section as possible to eliminate the effect of the accumulation of nitrogen pockets. Because the inlet pressure pickup contributed a small compressible volume to the system between the relocated flow restriction and the inlet of the test section, it was removed from the system, and no further attempts were made to measure the pressure drop across the test section. These modifications resulted in an increase in burnout flux of as high as 100 percent.

It was observed during additional check runs that the burnout heat flux still diminished somewhat as a function of running time. A sudden increase in heat flux was obtained when the accumulators were recharged with water; this indicated that nitrogen was leaking or diffusing through the bladders into the water.

The accumulators were changed from a parallel flow system to a series connection that eliminated any nitrogen from diffusing into the water flowing through the test section. The burnout heat fluxes obtained with this final arrangement were increased an additional 25 percent. The results were reproducible, and flow stability was implied from the steady wall-temperature recording immediately prior to the burnout transient.

In figure 3(b), the burnout heat fluxes obtained with the final arrangement of the apparatus are compared with results obtained in reference 3 with a flow system that was similar to the preliminary arrangement of the present investigation. The present results are 25 to 85 percent higher than those of reference 3; this indicates that the data of reference 3 were probably influenced by nitrogen diffusion and compressible volumes similar to those obtained in the present investigation with the original arrangement of the apparatus.

Compressible volume. - The effects of a compressible volume, located between the flow restriction and the inlet of the test section, on burnout heat flux and flow stability were briefly surveyed. The results are listed in table I and are shown graphically in figure 4. A sight glass was connected to the flow system at the test-section inlet as the volume source. With no heat addition in the test section, the flow rate was set at the desired rate. As the water level in the sight glass rose, the entrapped air was compressed to a pressure equivalent to the pressure drop across the test section. This compressible volume was adjusted to the desired value by venting the air to the atmosphere.

With heat addition, the pressure drop across the test section increased, and the compressible volume decreased accordingly. When boiling occurred in the test section, the liquid level in the sight glass fluctuated; this indicated large flow fluctuations in the test section. For mass-flow rates less than 0.6×10^6 pound per hour per square foot, the liquid level cycled slowly over the length of the sight glass as burnout was approached. The burnout flux varied over a wide range during the cycle, and the values plotted in figure 4 were measured while the water level in the sight glass was undergoing the least change in the cycle.

At higher flow rates, the burnout flux was more easily measured, and the magnitude of the level fluctuations was reduced by several orders. The frequency of the cycle changed from one cycle every 2 to 3 minutes to several cycles per minute.

In general, the results in figure 4 indicate that the burnout flux is reduced as the size of the compressible volume is increased and that a reduction of as much as 80 percent is obtained for a nominal value of compressible volume of 106 cubic centimeters.

The compressible volume installed in the system also approaches the case for flow in parallel channels connected to common headers and indicates that the burnout heat flux and flow stability would be greatly affected in parallel channels operating without a flow restriction in each channel.

Flow restriction. - The effect of varying the pressure drop across the flow restriction on burnout heat flux and flow stability was investigated. The final arrangement of the apparatus shown in figure 1(b) was used. The preheater power supply was not used, and the cables from the test-section power supply were connected to the inlet and the exit of the test section. The flow-restriction, or flow-rate-control, valves were located at the entrance to the test section. Separate test sections were fabricated for each length-to-diameter ratio investigated, so that the heated length of the test section corresponded to the hydrodynamic length. These burnout results are listed in table II and are shown graphically in figure 5.

In figure 5(a), the burnout heat flux is plotted against the pressure in the system upstream of the restriction for various test-section lengths and a constant flow rate of 1.78×10^6 pounds per hour per square foot. The pressure at the exit of the test section was atmospheric, so the gage pressure upstream of the restriction is equivalent to the pressure drop across the restriction and the test section.

The runs were conducted by setting a pressure upstream of the restriction of 800 pounds per square inch and then adjusting the flow-restriction valve to give the desired flow rate. As the burnout heat flux was approached, the pressure drop across the test section increased, and the flow valve was opened sufficiently to keep the flow rate constant. The procedure was repeated for lower pressures upstream of the restriction.

For the 50 L/D test section, the burnout heat flux was independent of the pressure drop across the restriction and the test section from 800 down to approximately 105 pounds per square inch. In this pressure-drop region, since the flow rate and the heat flux were constant, the pressure drop across the test section was constant, and the reduction in pressure drop corresponds to the reduction in pressure drop across the restriction.

When the pressure drop was reduced below 105 pounds per square inch, the resulting burnout heat flux was reduced, and the flow became unstable. For the lowest pressures, the flow rate fluctuated so much that the

burnout heat flux was difficult to define. In this low-pressure-drop region, the heat flux decreased, so the reduction in pressure drop corresponds to a reduction in pressure drop across the test section as well as the restriction.

The limit between stable- and unstable-flow burnout is indicated by the broken line faired through the knee of each curve (fig. 5(a)). The line represents the minimum pressure drops across the restriction and test section required for stable-flow burnout; these values are listed in the following table, together with other pertinent conditions:

Length-diameter ratio	Pressure drop across restriction and test section, lb/sq in.	Pressure drop across restriction, lb/sq in.	Pressure drop across test section, lb/sq in.	Burnout heat flux, $\frac{\text{Btu}}{(\text{hr})(\text{sq ft})}$	Exit quality
50	105	33	72	3.1×10^6	0.21
100	172	26	146	2.5	.43
150	217	31	186	2.0	.53
200	250	28	222	1.6	.59
250	260	31	229	1.3	.62

The part of the pressure drop due to the flow restriction could not be measured directly, since the pressure measuring system installed at the inlet of the test section introduced a slight compressible volume and resulted in flow instability at lower heat fluxes.

The minimum pressure drop across the restriction required to obtain flow stability was determined by a series of runs in which the burnout conditions at the knee of each curve (fig. 5(a)) were reproduced to determine the positions of the flow-restriction valve. After each valve setting was determined, the flow system was disconnected at the exit of the valve, and the pressure upstream of the valve was measured with the flow discharging to the atmosphere. With no pressure recovery assumed in the exit of the valve, the pressure drop across the valve is equivalent to the measured upstream pressure. A value of approximately 30 pounds per square inch was obtained for each of the various-length tubes.

The pressure drop across the test section can be acquired by subtracting the restriction pressure from the values of the minimum pressure drop across the restriction, and also from the test required for stable flow. The test-section pressure drop varied from 72 pounds per square inch for the 50 L/D tube to 229 for the 250 L/D tube. The independence of the restriction pressure drop for a 3-to-1 variation in the test-section pressure drop is unexplainable, inasmuch as both pressure drops occur upstream of the point of burnout.

Similar flow-stability tests, in which the flow rate was varied over a wide range, were made with a 50 L/D test section. The results are shown in figure 5(b). Burnout conditions at the flow-stability limit, indicated by the dashed line, are listed in the following table:

Flow rate, $\frac{lb}{(hr)(sq\ ft)}$	Pressure drop across restriction and test section, lb/sq in.	Pressure drop across restriction, lb/sq in.	Pressure drop across test section, lb/sq in.	Burnout heat flux, $\frac{Btu}{(hr)(sq\ ft)}$	Exit quality
0.13×10^6	12	5	7	0.5×10^6	0.56
.51	60	22	38	1.5	.47
1.78	108	33	75	3.1	.21
3.50	125	57	68	4.1	.10
5.85	137	85	52	5.3	.05
8.75	137	100	37	5.8	0

The values of the pressure drops across the restriction and the test section are plotted in figure 6 as a function of flow rate. The pressure drop across the restriction increased nearly linearly from 5 pounds per square inch at 0.13×10^6 pounds per hour per square foot to 100 pounds per square inch at a flow rate of 8.75×10^6 pounds per hour per square foot (0.5 to 40 ft/sec). The restriction pressure drop for a flow rate of 0.51×10^6 pounds per hour per square foot was ignored in fairing the curve. The test-section pressure drop increased rapidly at first with flow rate and then decreased at the higher flow rates because of the reduction in exit quality, with the maximum value occurring at a flow rate less than approximately 1×10^6 pounds per hour per square foot. The data are insufficient to determine the flow rate at which the maximum test-section pressure drop occurred.

Effects of Tube Geometry and Flow Conditions on Burnout in Stable-Flow Region

Typical high-quality burnout conditions. - The wall-temperature variation along the length of the tube for a typical burnout with high exit quality is shown in figure 7. The outer wall temperature reached a maximum value approximately one-fourth the distance from the inlet. At the exit of the tube, the wall temperature fluctuated about 20° F just prior to burnout.

For constant heat addition along the tube, the quality and pressure distribution along the length were calculated by iteration; the resulting

values are shown in figure 7. The water temperature increases linearly in the first quarter of the tube until the saturation value is obtained. In the remaining length, the saturation temperature decreases with the decrease in pressure along the length. The estimated inner-wall temperature decreases with the decrease in saturation temperature; hence, the difference between the wall temperature and the saturation temperature is nearly constant for the remaining three-fourths length of the tube.

Tube diameter and length. - Burnout conditions in the stable-flow region were determined for a range of tube diameters from 0.051 to 0.188 inches and length-to-diameter ratios from 25 to 250. Each geometry was investigated over a flow-rate range from approximately 0.1 to 2.5×10^6 pounds per hour per square foot, or to a maximum value corresponding to the maximum voltage available from the electric-power supply. The flow-rate range was extended to 25×10^6 pounds per hour per square foot for a tube diameter of 0.051 inch and length-to-diameter ratios of 50 and 250 by using thick-walled test sections. The results are listed in table III.

Representative variations of burnout heat flux with flow rate and length-to-diameter ratio are shown in figure 8 for a tube diameter of 0.051 inch. In the low-flow-rate range, the burnout flux varies directly as the flow rate to the 0.85 power and inversely as the length-to-diameter ratio to the 0.85 power. In the high-flow-rate region, the heat flux varies directly as the flow rate to the 0.5 power and inversely as the length-to-diameter ratio to the 0.6 power.

A maximum value of heat flux of 13.2×10^6 Btu per hour per square foot was obtained with the 50 L/D tube at a mass flow of 25×10^6 pounds per hour per square foot. This corresponds to an inlet velocity of about 98 feet per second.

A comparison of the data from table III for constant values of length-to-diameter ratio and mass flow indicates that the burnout heat flux varies inversely as the tube diameter to the 0.2 power in the low-velocity region and approximately to the 0.5 power at the higher velocities.

The effect of tube geometry on burnout is shown in figure 9. All the data from table III for the various tube geometries are compared in figure 9(a), where the parameter $(Q/S)\ (D)^{0.2}\ (L/D)^{0.85}$ is plotted against the flow rate G for the Btu-pound-foot-hour system of units. The data corresponding to burnout at high exit qualities are well represented by the solid line with a slope of 0.85. For lower quality burnout, the data break away from the solid line at flow rates of approximately 0.09, 0.4, 1.5, and 5×10^6 pounds per hour per square foot for the 25, 50, 100, and 250 L/D tubes, respectively. The slope of the dashed lines is 0.5. The scatter in the data for the 50 L/D test section is due in part to an increase in the effect of tube diameter on burnout heat flux.

In figure 9(b), the separation of the low-quality burnout data with the length-to-diameter ratio is eliminated by dividing the ordinate parameter by $(L/D)^{1.7}$ and the flow rate by $(L/D)^2$. The correlation of the data for high exit qualities is not affected, since the slope of the line in this region is 0.85. The data are well represented by the relation

$$(Q/S)\ D^{0.2}\ (L/D)^{0.85} = 270\ G^{0.85} \qquad (1)$$

for values of $G/(L/D)^2$ less than 150.

The data for the low-quality burnout is represented by the relation

$$(Q/S)\ D^{0.2}\ (L/D)^{0.15} = 1400\ G^{0.5} \qquad (2)$$

for values of $G/(L/D)^2$ greater than 150.

The wider separation of the data in this region, as mentioned previously, could be reduced somewhat by raising the diameter in the ordinate term to the 0.4 or 0.6 power instead of the 0.2 power. The range of conditions does not overlap sufficiently to define fully the diameter effect in this region.

The data for values of $G/(L/D)^2$ near 150 were examined to see if there was any particular reason for the parameter being a distinguishing limit on burnout regions. The exit quality varied from approximately 40 percent for the 0.188-inch-diameter tubes to 60 percent for the 0.051-inch-diameter tubes.

The tube wall temperatures at the exit of the test section varied too inconsistently to be of any use in distinguishing between the high- and low-quality burnout regions.

It was noted in the flow-restriction tests shown in figure 6 that the pressure drop across the test section for a 50 L/D tube increased with an increase in flow rate to a maximum value for a flow rate of approximately 1×10^6 pounds per hour per square foot and then decreased with a further increase in flow rate. This value of flow rate for which the pressure drop is a maximum roughly compares with a flow rate of 0.6×10^6 pounds per hour per square foot for the limit of the two burnout regions for a 50 L/D tube and suggests an interrelation between test-section pressure drop and burnout regimes.

Data from reference 4 for flow in a circular tube with a diameter of 0.94 inch and length-to-diameter ratios of 8.5 to 36 and in a rectangular channel with an equivalent diameter of 0.168 and a length-to-diameter ratio of 256 are compared with equations (1) and (2) of this report in

figure 9(c). The data are in good agreement with the present results and indicate that the effect of diameter on burnout in the low-flow-rate region is applicable for tube diameters up to 1 inch.

Effect of variation of inlet temperature and exit pressure on burnout. - Preliminary runs were made to determine whether the length of the tube used for preheating had any effect on burnout in the test section. The total heat supplied by the preheater was held constant while the heat flux was increased by moving the downstream cable clamp nearer the inlet of the tube. Burnout in the test section was not affected by the heat flux in the preheater up to the condition of burnout in the preheater.

The effect of preheating on the burnout flux is shown in figure 10. The ratio of burnout flux at the inlet preheating temperature to the burnout flux at a reference temperature of 70° F is plotted against the temperature difference between the inlet preheating temperature and outlet saturation temperature. The data in figure 10 are tabulated in table IV. As the inlet water temperature is increased from 70° to 212° F, the burnout flux is reduced by as much as 20 percent. Figure 10 also indicates a considerable increase in scatter of data over this temperature range with increased preheating. This scatter is primarily due to the difficulty in accurately controlling the degree of preheating of the water and to the introduction of instability effects into the system from steam bubbles generated in the preheater.

The effect of back pressure on the burnout flux is shown in figure 11, where the ratio of the burnout flux at a given exit pressure to the burnout flux at atmospheric pressure is plotted against the mass-flow rate. For the limited back pressures used, 50 and 100 pounds per square inch, the burnout flux increased with increasing back pressure over the values at atmospheric exit pressure by as much as 15 percent at 100 pounds per square inch.

SUMMARY OF RESULTS

Boiling burnout was investigated for water flowing vertically upward through electrically heated tubes with a flow-restricting valve located before the test section; this water was then discharged into a compressible-volume tank. The effects of flow-system characteristics on flow stability and burnout were briefly surveyed. For stable-flow conditions, burnout was determined for tube diameters ranging from 0.051 to 0.188 inch, length-to-diameter ratios of 25 to 250; flow rates from 0.02 to 25×10^6 pounds per hour per square foot (0.1 to 98 ft/sec), inlet

water temperatures of 72° to 212° F, and discharge pressures ranging from 0 to 100 pounds per square inch. The results may be summarized as follows:

1. Maximum values of burnout heat flux were obtained for stable flow by restricting the flow upstream of the test section. The minimum pressure drop across the restriction required to stabilize the flow increased from 5 to 100 pounds per square inch when the inlet flow velocity was increased from 0.5 to 40 feet per second.

2. A compressible volume introduced in the flow system between the flow restriction and the inlet of the test section resulted in unsteady flow during burnout. The flow fluctuations increased and the burnout heat flux decreased with an increase in the compressible volume.

3. Nitrogen in the water produced results similar to those obtained with a compressible volume at the test-section inlet.

4. For stable-flow conditions, net steam was generated at burnout. Two regimes of burnout were obtained. In the low-velocity high-exit-quality region, the data were correlated by the relation

$$(Q/S)\ D^{0.2}\ (L/D)^{0.85} = 270\ G^{0.85} \text{ for } G/(L/D)^2 < 150$$

and in the high-velocity low-exit-quality region by

$$(Q/S)\ D^{0.2}\ (L/D)^{0.15} = 1400\ G^{0.5} \text{ for } G/(L/D)^2 > 150$$

where Q/S is the heat flux, D is the inside tube diameter, L/D is the length-to-diameter ratio, and G is the mass-flow rate.

5. At the limiting value of $G/(L/D)^2$ of 150, the exit quality varied from 40 to 60 percent.

6. The burnout heat flux was decreased by as much as 20 percent for an increase in water inlet temperature from 70° to 212° F.

7. An increase in exit pressure from atmospheric pressure to 100 pounds per square inch resulted in an increase in burnout flux of approximately 15 percent.

Lewis Flight Propulsion Laboratory
National Advisory Committee for Aeronautics
Cleveland, Ohio, August 1, 1958

REFERENCES

1. Kreith, Frank, and Foust, Alan S.: Remarks on the Mechanism and Stability of Surface-Boiling Heat Transfer. Paper No. 54-A-146, ASME, 1954.

2. Clark, John A., and Rohsenow, Warren M.: Local Boiling Heat Transfer to Water at Low Reynolds Numbers and High Pressures. Trans. ASME, vol. 76, no. 4, May 1954, pp. 553-562.

3. Lowdermilk, Warren H., and Weiland, Walter F.: Some Measurements of Boiling Burn-Out. NACA RM E54K10, 1955.

4. Jens, W. H., and Lottes, P. A.: Two-Phase Pressure Drop and Burnout Using Water Flowing in Round and Rectangular Channels. ANL-4915, Argonne Nat. Lab., Oct. 1, 1952. (Contract W-31-109-eng-38.)

TABLE I. - EFFECT OF COMPRESSIBLE VOLUME ON BURNOUT

[Tube diameter, 0.096 in.; length-diameter ratio, 100; exit pressure, atmospheric; pressure upstream of restriction, 300 lb/sq in.]

Run	Compressible volume, cc	Water inlet temperature, °F	Mass flow, $\frac{G}{10^6}$, $\frac{lb}{(hr)(sq\ ft)}$	Burnout heat flux, $\frac{Q/S}{10^6}$, $\frac{Btu}{(hr)(sq\ ft)}$
101	0	72	0.75	1.32
102	66	↓	↓	.42
103	72	↓	↓	.35
104	84	↓	↓	.32
105	104	↓	↓	.28
106	122	↓	↓	.31
107	144	↓	↓	.28
108	106	↓	↓	.32
109	↓	↓	.050	.11
110	↓	↓	.068	.17
111	↓	↓	.10	.17
112	↓	↓	.15	.21
113	↓	↓	.19	.22
114	↓	↓	.40	.22
115	↓	↓	.75	.32
116	↓	↓	1.02	.36
117	↓	↓	1.49	.45
118	↓	↓	1.90	.57
119	↓	↓	2.54	.73
120	↓	↓	4.00	1.20
121	↓	↓	5.95	1.73
122	↓	↓	9.60	4.12
123	↓	↓	7.86	2.95
124	↓	↓	2.92	.92

TABLE II. - EFFECT OF FLOW RESTRICTION ON BURNOUT

[Tube diameter, 0.076 in.; exit pressure, atmospheric.]

Run	Length-diameter ratio	Water inlet temperature, °F	Pressure upstream of restriction, lb/sq in.	Mass flow, $\frac{G}{10^6}$, $\frac{lb}{(hr)(sq\ ft)}$	Burnout heat flux, $\frac{Q/S}{10^6}$, $\frac{Btu}{(hr)(sq\ ft)}$
125	250	74	400	1.78	1.32
126	↓	↓	360	↓	1.32
127			340		1.32
128			320		1.32
129			300		1.32
130			275		1.32
131			250		1.25
132			242		1.24
133			235		1.22
134			225		1.19
135			200		1.03
136			150		.80
137			100		.546
138	↓		60		.374
139	200		275		1.58
140	↓		250		1.58
141			245		1.56
142			240		1.54
143			220		1.46
144			175		1.14
145			125		.825
146			100		.66
147	↓		60		.538
148	150		250		1.96
149	↓		225		1.98
150			215		1.93
151			211		1.91
152			200		1.79
153			110		.99
154	↓	↓	55	↓	.56

TABLE II. - Continued. EFFECT OF FLOW RESTRICTION ON BURNOUT

[Tube diameter, 0.076 in.; exit pressure, atmospheric.]

Run	Length-diameter ratio	Water inlet temperature, °F	Pressure upstream of restriction, lb/sq in.	Mass flow, $\frac{G}{10^6}$, $\frac{lb}{(hr)(sq\ ft)}$	Burnout heat flux, $\frac{Q/S}{10^6}$, $\frac{Btu}{(hr)(sq\ ft)}$
155	100	74	255	1.78	2.52
156			250		2.43
157			240		2.48
158			225		2.52
159			220		2.45
160			210		2.53
161			200		2.47
162			190		2.53
163			180		2.50
164			170		2.49
165			163		2.28
166			160		2.30
167			140		2.07
168			120		1.69
169			100		1.49
170			55		.92
171	50		215		3.10
172			150		3.04
173			125		3.10
174			110		3.10
175			102		3.00
176			100		2.98
177			75		2.4
178			60		2.14
179			40		1.39
180			66	.127	.468
181			45		.48
182			33		.433
183			17		.406
184			12		.467
185			9		.432
186			5		.390
187			2.5		.358

TABLE II. - Concluded. EFFECT OF FLOW RESTRICTION ON BURNOUT

[Tube diameter, 0.076 in.; exit pressure, atmospheric.]

Run	Length-diameter ratio	Water inlet temperature, °F	Pressure upstream of restriction, lb/sq in.	Mass flow, $\frac{G}{10^6}$, $\frac{lb}{(hr)(sq\ ft)}$	Burnout heat flux, $\frac{Q/S}{10^6}$, $\frac{Btu}{(hr)(sq\ ft)}$
188	50	74	100	0.509	1.5
189	↓	↓	70	↓	1.5
190			60		1.5
191			55		1.44
192			45		1.35
193			20		.981
194			200	3.5	4.12
195			150	↓	4.12
196			135		4.12
197			128		4.12
198			125		4.12
199			110		3.88
200			75		3.4
201			50		2.84
202			225	5.85	5.3
203			175	↓	5.3
204			140		5.3
205			137		5.2
206			125		5.17
207			110		5.1
208			75		4.56
209			50		3.65
210			200	8.75	5.79
211			165	↓	5.79
212			140		5.79
213			135		5.83
214			130		5.69
215			110		5.6
216			75		5.3
217	↓	↓	50	↓	4.8

TABLE III. - EFFECT OF TUBE GEOMETRY ON BURNOUT

[Exit pressure, atmospheric.]

Run	Tube diameter, in.	Length-diameter ratio	Water inlet temperature, °F	Pressure upstream of restriction, lb/sq in.	Mass flow, $\frac{G}{10^6}$, $\frac{lb}{(hr)(sq\ ft)}$	Burnout heat flux, $\frac{Q/S}{10^6}$, $\frac{Btu}{(hr)(sq\ ft)}$	Exit quality
220	0.051	50	74	250	0.11	0.55	0.88
221					.22	.99	.77
222					.50	1.60	.52
223					.70	1.86	.41
224					.99	2.46	.36
225					1.51	3.19	.29
226					1.88	3.95	.29
227					2.32	4.35	.24
228					2.81	4.65	.20
229			78	750	4.39	6.19	.15
230					5.45	6.85	.12
231					7.95	7.94	.07
232					12.2	8.60	.07
233					19.4	11.1	----
234					25.2	13.2	----
235		100	74	250	.11	.31	.97
236					.20	.54	.95
237					.41	.92	.78
238					.51	1.09	.75
239					.70	1.39	.68
240					1.03	2.07	.68
241				400	1.51	2.68	.59
242					1.84	3.22	.57
243					2.39	3.66	.48
244					2.84	3.86	.41
245					3.77	4.45	.34
246		150		250	.11	.22	1.0+
247					.20	.36	.96
248					.42	.66	.83
249					.51	.79	.81
250			72	400	.71	1.01	.73
251					.99	1.42	.74
252					1.47	1.91	.66
253					1.91	2.50	.66
254					2.38	2.81	.59

TABLE III. - Continued. EFFECT OF TUBE GEOMETRY ON BURNOUT

Run	Tube diameter, in.	Length-diameter ratio	Water inlet temperature, °F	Pressure upstream of restriction, lb/sq in.	Mass flow, $\frac{G}{10^6}$, $\frac{lb}{(hr)(sq\ ft)}$	Burnout heat flux, $\frac{Q/S}{10^6}$, $\frac{Btu}{(hr)(sq\ ft)}$	Exit quality
255	0.051	200	74	250	0.11	0.16	1.0+
256					.19	.26	.98
257					.38	.46	.86
258			72	400	.50	.56	.78
259					.70	.80	.79
260					1.03	1.12	.75
261					1.49	1.54	.70
262					1.78	1.90	.74
263					2.38	2.23	.63
264		250	74	250	.11	.14	1.0+
265					.19	.22	1.0+
266					.41	.40	.87
267				300	.50	.48	.84
268					.70	.66	.83
269					.99	.88	.78
270					1.38	1.11	.68
271					1.84	1.29	.57
272			78	700	4.6	2.86	.50
273				700	5.67	3.36	.47
274				800	6.80	3.80	.44
275				850	8.07	4.09	.37
276				870	9.7	4.45	.33
277				920	11.3	4.91	.30
278				930	12.9	5.37	.28
279				950	15.0	5.75	.25
280					16.1	6.16	.25
281					18.7	6.66	.22
282					22.4	7.40	.20
283	.076	50	74	350	.25	1.00	.69
284					.30	1.09	.61
285					.38	1.32	.57
286					.51	1.52	.48
287					.71	1.82	.38
287					.99	2.65	.41
288					1.48	3.20	.31
289					1.95	3.63	.24
290					2.52	3.76	.17
291					3.04	4.16	.14
292			78		8.75	5.90	----

TABLE III. - Continued. EFFECT OF TUBE GEOMETRY ON BURNOUT

[Exit Pressure, atmospheric.]

Run	Tube diameter, in.	Length-diameter ratio	Water inlet temperature, °F	Pressure upstream of restriction, lb/sq in.	Mass flow, $\frac{G}{10^6}$, $\frac{lb}{(hr)(sq\ ft)}$	Burnout heat flux, $\frac{Q/S}{10^6}$, $\frac{Btu}{(hr)(sq\ ft)}$	Exit quality
293	0.076	100	76	350	0.13	0.29	0.73
294					.19	.46	.87
295					.31	.65	.72
296					.38	.78	.71
297					.52	1.02	.66
298					.71	1.34	.64
299					1.00	1.91	.64
300					1.51	2.46	.53
301					1.97	2.80	.45
302					2.50	3.23	.39
303					3.04	3.53	.34
304					3.46	3.74	.31
305		↓		↓	4.91	4.30	.22
306		150		400	.11	.17	.87
307					.16	.27	.94
308					.31	.46	.79
309					.39	.55	.75
310					.51	.74	.76
311					.71	.95	.52
312					.98	1.30	.67
313					1.51	1.75	.58
314					1.94	2.16	.55
315					2.51	2.60	.50
316		↓	↓	↓	3.08	2.94	.45
317		200	73	350	.10	.12	.82
318					.16	.20	.88
319					.30	.33	.76
320					.38	.42	.76
321					.51	.54	.73
322					.71	.73	.70
323					1.03	1.05	.70
324					1.60	1.47	.60
325					1.95	1.78	.61
326	↓	↓	↓	↓	2.44	2.01	.54

TABLE III. - Continued. EFFECT OF TUBE GEOMETRY ON BURNOUT

[Exit pressure, atmospheric.]

Run	Tube diameter, in.	Length-diameter ratio	Water inlet temperature, °F	Pressure upstream of restriction, lb/sq in.	Mass flow, $\frac{G}{10^6}$, $\frac{lb}{(hr)(sq\ ft)}$	Burnout heat flux, $\frac{Q/S}{10^6}$, $\frac{Btu}{(hr)(sq\ ft)}$	Exit quality
327	0.076	250	73	350	0.051	0.061	1.0+
328					.098	.092	.82
329					.16	.15	.82
330					.30	.25	.71
331					.38	.34	.78
332					.52	.46	.77
333					.70	.59	.72
334					1.00	.81	.69
335					1.52	1.16	.64
336					1.77	1.29	.61
337					1.88	1.34	.59
338	.096	50	76		.25	.92	.63
339					.30	1.07	.59
340					.40	1.20	.49
341					.53	1.35	.40
342					.70	1.77	.38
343					.99	2.16	.33
344					1.49	3.00	.28
345					1.90	3.35	.23
346					2.48	3.61	.16
347					3.05	4.04	.14
348					3.57	4.32	.11
349					4.03	4.73	.10
350					4.94	5.16	.08
351					5.95	5.24	.04
352					5.95	5.44	.05
353					7.93	6.00	.02
354					9.95	7.82	.02
355		100		300	.14	.31	.78
356					.24	.50	.71
357					.30	.61	.70
358					.40	.78	.67
359					.50	.94	.64
360					.69	1.27	.62
361					.99	1.76	.60
362					1.48	2.23	.49
363					1.91	2.66	.44
364					2.53	3.02	.36
365					3.05	3.38	.32
366					3.49	3.67	.30
367					3.90	3.96	.28

TABLE III. - Continued. EFFECT OF TUBE GEOMETRY ON BURNOUT

[Exit pressure, atmospheric.]

Run	Tube diameter, in.	Length-diameter ratio	Water inlet temperature, °F	Pressure upstream of restriction, lb/sq in.	Mass flow, $\frac{G}{10^6}$, $\frac{lb}{(hr)(sq\ ft)}$	Burnout heat flux, $\frac{Q/S}{10^6}$, $\frac{Btu}{(hr)(sq\ ft)}$	Exit quality
368	0.096	150	76	300	0.10	0.17	0.92
369					.19	.28	.78
370					.30	.42	.74
371					.41	.57	.72
372					.54	.70	.67
373				350	.69	.91	.67
374					.99	1.21	.62
375					1.50	1.71	.57
376					1.91	2.08	.53
377					2.77	2.48	.42
378		200			.070	.078	.79
379					.12	.13	.79
380					.20	.23	.82
381					.29	.32	.78
382					.40	.43	.77
383					.51	.51	.70
384					.70	.72	.71
385					1.00	.93	.64
386					1.51	1.32	.59
387					2.07	1.70	.55
388		250			.074	.073	.88
389					.12	.11	.81
390					.19	.18	.81
391					.30	.28	.82
392					.40	.34	.73
393					.51	.41	.70
394					.70	.57	.71
395					1.01	.77	.64
396					1.53	1.09	.60
397					1.83	1.24	.56
398	.123	25	74	300	.044	.47	.94
399					.074	.72	.83
400					.107	.87	.68
401					.15	1.18	.63
402					.20	1.27	.49

TABLE III. - Continued. EFFECT OF TUBE GEOMETRY ON BURNOUT

[Exit pressure, atmospheric.]

Run	Tube diameter, in.	Length-diameter ratio	Water inlet temperature, °F	Pressure upstream of restriction, lb/sq in.	Mass flow, $\frac{G}{10^6}$, $\frac{lb}{(hr)(sq\ ft)}$	Burnout heat flux, $\frac{Q/S}{10^6}$, $\frac{Btu}{(hr)(sq\ ft)}$	Exit quality
403	0.123	25	74	300	0.21	1.26	0.46
404					.28	1.51	.40
405					.41	1.80	.30
406					.50	1.91	.24
407					.69	2.08	.16
408					1.02	2.37	.09
409					3.03	3.65	0
410					3.55	4.07	0
411			78	1100	1.87	3.27	.04
412			78	1100	1.04	2.62	.11
413		50	74	300	.020	.15	1.0+
414					.044	.26	1.0+
415					.075	.40	.94
416					.107	.48	.76
417					.16	.70	.76
418					.20	.82	.67
419					.28	.96	.54
420					.34	1.13	.53
421					.50	1.38	.42
422					.69	1.43	.27
423					1.01	1.99	.25
424					1.33	2.26	.20
425					1.94	2.64	.13
426					2.58	2.95	.09
427					3.06	3.26	.07
428					3.60	3.54	.05
429			78	1100	4.29	3.78	.04
430			78	1100	1.84	2.68	.16
431		100	74	300	.075	.20	.94
432					.11	.28	.85
433					.16	.39	.85
434					.20	.45	.75
435					.28	.58	.70
436					.42	.87	.70
437					.50	.99	.66
438					.69	1.22	.56

TABLE III. - Continued. EFFECT OF TUBE GEOMETRY ON BURNOUT

[Exit pressure, atmospheric.]

Run	Tube diameter, in.	Length-diameter ratio	Water inlet temperature, °F	Pressure upstream of restriction, lb/sq in.	Mass flow, $\frac{G}{10^6}$, $\frac{lb}{(hr)(sq\ ft)}$	Burnout heat flux, $\frac{Q/S}{10^6}$, $\frac{Btu}{(hr)(sq\ ft)}$	Exit quality
439	0.123	100	74	300	1.06	1.67	0.49
440					1.33	1.95	.45
441					1.94	2.34	.34
442					2.57	2.76	.29
443					3.03	2.99	.25
444					3.74	3.30	.21
445		150		250	.051	.11	1.0+
446					.10	.17	.87
447					.20	.30	.75
448				300	.27	.40	.73
449					.39	.55	.70
450					.52	.74	.72
451					.67	.90	.66
452					1.08	1.33	.60
453					1.33	1.55	.56
454					1.65	1.75	.50
455		200			.11	.14	.89
456					.16	.20	.88
457					.20	.25	.87
458					.28	.32	.78
459					.40	.44	.75
460					.51	.56	.74
461					.70	.68	.64
462					1.10	1.02	.60
463	.156	25			.062	.52	.72
464					.10	.72	.59
465					.15	.87	.45
466					.20	1.04	.38
467					.31	1.20	.26
468					.42	1.37	.19
469					.50	1.49	.16
470		50	76		.056	.22	.64
471					.10	.37	.61
472					.15	.51	.54
473					.20	.64	.52
474					.29	.82	.43

TABLE III. - Continued. EFFECT OF TUBE GEOMETRY ON BURNOUT

[Exit pressure, atmospheric.]

Run	Tube diameter, in.	Length-diameter ratio	Water inlet temperature, °F	Pressure upstream of restriction, lb/sq in.	Mass flow, $\frac{G}{10^6}$, $\frac{lb}{(hr)(sq\ ft)}$	Burnout heat flux, $\frac{Q/S}{10^6}$, $\frac{Btu}{(hr)(sq\ ft)}$	Exit quality
475	0.156	50	74	300	0.71	1.51	0.30
476					.99	1.74	.22
477					1.54	2.22	.15
478					2.03	2.34	.09
479					2.53	2.68	.07
480					3.01	2.86	.05
481					.060	.25	.68
482					.10	.38	.63
483					.16	.52	.53
484					.20	.62	.49
485					.28	.77	.43
486					.51	1.16	.32
487					.60	1.35	.32
488					.55	1.21	.30
489					.51	1.11	.31
490					.48	1.07	.32
491					.20	.63	.50
492					.70	1.56	.31
493					1.02	1.71	.20
494					1.64	2.14	.12
495				250	2.00	2.23	.08
496					3.14	2.72	.03
497					3.58	3.02	.03
498				1100	2.76	2.67	.06
499		100	76	300	.057	.14	.84
500					.105	.24	.79
501					.15	.31	.70
502					.20	.42	.73
503					.31	.57	.62
504					.40	.71	.58
505					.50	.86	.55
506					.72	1.13	.50
507					1.01	1.45	.45
508					1.21	1.66	.42
509		150	73	250	.057	.095	.88
510					.10	.16	.81
511					.15	.22	.75

TABLE III. - Continued. EFFECT OF TUBE GEOMETRY ON BURNOUT

[Exit pressure, atmospheric.]

Run	Tube diameter, in.	Length-diameter ratio	Water inlet temperature, °F	Pressure upstream of restriction, lb/sq in.	Mass flow, $\frac{G}{10^6}$, $\frac{lb}{(hr)(sq\ ft)}$	Burnout heat flux, $\frac{Q/S}{10^6}$, $\frac{Btu}{(hr)(sq\ ft)}$	Exit quality
512	0.156	150	70	250	0.19	0.27	0.71
513					.30	.38	.63
514					.40	.48	.60
515					.51	.60	.58
516					.73	.83	.56
517		200			.058	.062	.74
518					.10	.11	.76
519					.16	.17	.72
520					.18	.20	.75
521			71		.30	.29	.64
522					.40	.36	.60
523					.52	.46	.58
524			73		.53	.47	.59
525					.15	.16	.75
526					.059	.053	.78
527		250	71		.058	.062	.95
528					.10	.10	.89
529					.15	.14	.80
530					.20	.18	.81
531					.31	.26	.72
532					.31	.26	.74
533					.31	.25	.70
534					.31	.28	.79
535	.188	25	74		.020	.14	.59
536					.030	.23	.65
537					.040	.31	.65
538					.070	.47	.54
539					.15	.80	.40
540					.21	.99	.35
541					.30	1.08	.22
542					.40	1.31	.19
543					.50	1.46	.16
544			72		.10	.66	.51
545					.050	.34	.56
546		50			.030	.13	.72
547					.050	.26	.78
548					.070	.30	.74

TABLE III. - Concluded. EFFECT OF TUBE GEOMETRY ON BURNOUT

[Exit pressure, atmospheric.]

Run	Tube diameter, in.	Length-diameter ratio	Water inlet temperature, °F	Pressure upstream of restriction, lb/sq in.	Mass flow, $\frac{G}{10^6}$, $\frac{lb}{(hr)(sq\ ft)}$	Burnout heat flux, $\frac{Q/S}{10^6}$, $\frac{Btu}{(hr)(sq\ ft)}$	Exit quality
549	0.188	50	75	250	0.101	0.38	0.63
550					.15	.48	.49
551					.20	.60	.46
552					.30	.78	.39
553					.40	.95	.34
554					.50	1.10	.31
555					.70	1.45	.28
556					.70	1.32	.25
557			72		.70	1.32	.25
558		100	75		.051	.14	.99
559					.10	.24	.83
560					.15	.33	.74
561					.21	.42	.69
562					.30	.53	.58
563					.40	.68	.55
564					.49	.82	.54
565					.52	.84	.53
566					.69	1.04	.48
567					1.02	1.43	.43
568					1.76	2.04	.33
569		150	72		.051	.097	1.0+
570			72		.10	.17	.89
571			76		.15	.22	.77
572					.20	.28	.71
573					.30	.37	.63
274					.41	.49	.60
575					.49	.58	.59
576					.70	.79	.55
577					.69	.77	.55
578					1.04	1.12	.53
579		200			.051	.086	1.0+
580					.15	.20	.93
581					.20	.22	.75
582					.30	.30	.68
583					.40	.38	.63
584					.50	.47	.64
585					.70	.59	.55
586					.81	.63	.49
587					.10	.10	.89

TABLE IV. - EFFECT OF INLET TEMPERATURE ON BURNOUT

[Exit pressure, atmospheric; pressure upstream of restriction, 300 lb/sq in.]

Run	Tube diameter, in.	Length-diameter ratio	Water inlet temperature, °F	Mass flow, $\frac{G}{10^6}$, $\frac{lb}{(hr)(sq\ ft)}$	Burnout heat flux, $\frac{Q/S}{10^6}$, $\frac{Btu}{(hr)(sq\ ft)}$	Exit quality
588	0.096	200	72	0.44	0.48	0.75
589			90	.45	.47	.77
590			104	.45	.48	.78
591			112	.43	.44	.70
592			125	.43	.46	.78
593			138	.43	.46	.79
594			146	.44	.45	.78
595			166	.44	.44	.78
596			175	.44	.44	.79
597			186	.44	.43	.79
598			198	.44	.42	.78
599			210	.44	.42	.78
600		50	114	.43	1.23	.52
601			169	.43	1.34	.59
602			208	.43	1.21	.57
603			72	.98	2.46	.37
604			112	.98	2.46	.41
605			160	.98	2.46	.46
606			200	.98	2.44	.50
607			72	.42	1.32	.22
608			72	1.92	3.44	.27
609			118	1.92	3.44	.33
610			174	1.92	3.44	.37
611			212	1.92	3.44	.44
612		100	72	1.92	2.73	.47
613			120	1.92	2.66	.52
614			182	1.92	2.56	.54
615			200	1.92	2.56	.69
616			212	.99	1.67	.64
617			170	.99	1.67	.63
618			120	.99	1.75	.63
619			72	.99	1.80	.60
620			70	.43	.88	.69
621			126	.43	.86	.73
622			170	.43	.84	.76
623			205	.43	.83	.77
624		200	70	1.01	.98	.65
625			120	1.01	.92	.66
626			170	1.00	.87	.67
627			212	1.01	.81	.66
628			70	1.75	1.56	.59
629			127	1.69	1.47	.63
630			162	1.68	1.35	.61
631			212	1.67	1.29	.64

TABLE IV. - Concluded. EFFECT OF INLET TEMPERATURE ON BURNOUT

[Exit pressure, atmospheric; pressure upstream of restriction, 300 lb/sq in.]

Run	Tube diameter, in.	Length-diameter ratio	Water inlet temperature, °F	Mass flow, $\frac{G}{10^6}$, $\frac{lb}{(hr)(sq\ ft)}$	Burnout heat flux, $\frac{Q/S}{10^6}$, $\frac{Btu}{(hr)(sq\ ft)}$	Exit quality
632	0.051	100	70	1.02	1.85	0.61
633			123	1.02	1.81	.65
634			174	1.02	1.80	.69
635			205	1.02	1.78	.72
636			125	.70	1.24	.64
637			170	.70	1.23	.68
638			200	..71	1.33	.76
639			80	.71	1.41	.69
640			72	2.37	2.82	.48
641			132	2.41	2.70	.45
642			172	2.45	2.52	.42
643			204	2.45	2.42	.40
644		200	72	1.57	1.49	.64
645			140	1.57	1.36	.64
646			176	1.57	1.37	.69
647			212	1.55	1.22	.65
648			212	1.03	.79	.63
649			180	1.02	.78	.72
650			130	1.00	.88	.64
651			80	1.00	1.05	.73
652			72	.12	.18	1.0+
653			110	.12	.15	.89
654		50	188	.49	1.61	.66
655			149	.49	1.61	.61
656			114	.49	1.76	.62
657			80	.49	1.64	.56
658			70	.99	2.35	.34
659			120	.99	2.99	.52
660			160	.99	2.99	.57
661			185	.99	3.19	.64
662			80	2.02	3.20	.19
663			112	2.09	3.36	.23
664			200	2.09	3.22	.31

TABLE V. - EFFECT OF EXIT PRESSURE ON BURNOUT

[Tube diameter, 0.096 in.; water inlet temperature, 72° F; pressure upstream of restriction, 300 lb/sq in.]

Run	Length-diameter ratio	Exit pressure, lb/sq in.	Mass flow, $\frac{G}{10^6}$, $\frac{lb}{(hr)(sq\ ft)}$	Burnout heat flux, $\frac{Q/S}{10^6}$, $\frac{Btu}{(hr)(sq\ ft)}$	Exit quality
665	100	0	0.20	0.43	0.76
666			.51	.94	.62
667			1.00	1.62	.53
668			1.48	2.17	.46
669		50	.48	.95	.63
670			1.00	1.65	.47
671			1.48	2.18	.40
672			.20	.46	.87
673		100	.20	.49	.84
674			.48	1.09	.74
675			1.01	1.74	.48
676			1.48	2.22	.38
677	200	0	.20	.24	.83
678			.53	.54	.69
679			1.00	.95	.64
680			1.48	1.26	.55
681		50	.48	.54	.74
682			.99	.90	.56
683			1.47	1.26	.51
684			.20	.26	.91
685		100	.19	.25	.90
686			.48	.58	.81
687			1.00	.98	.60
688			1.48	1.32	.51

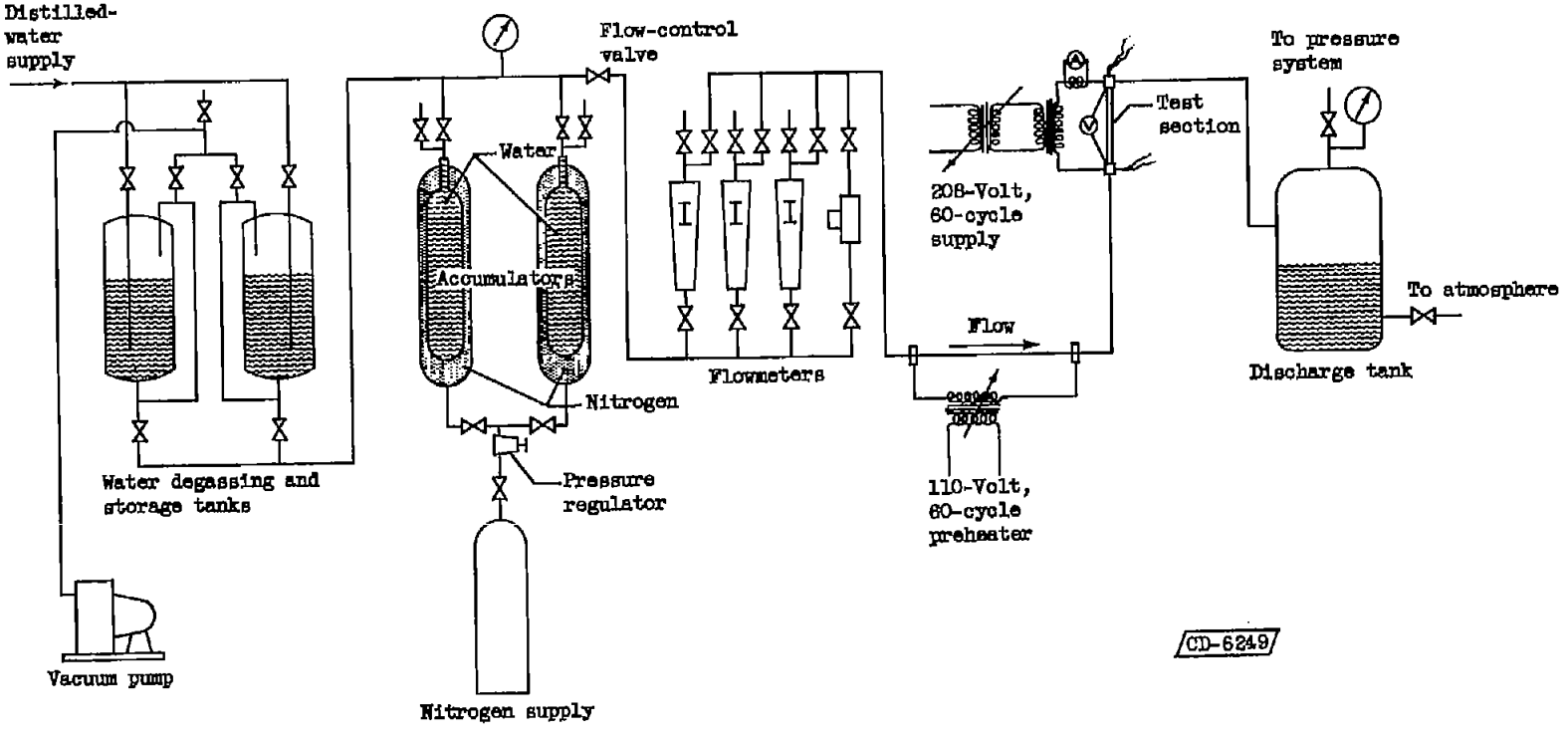

(a) Preliminary.

Figure 1. - Arrangement of apparatus.

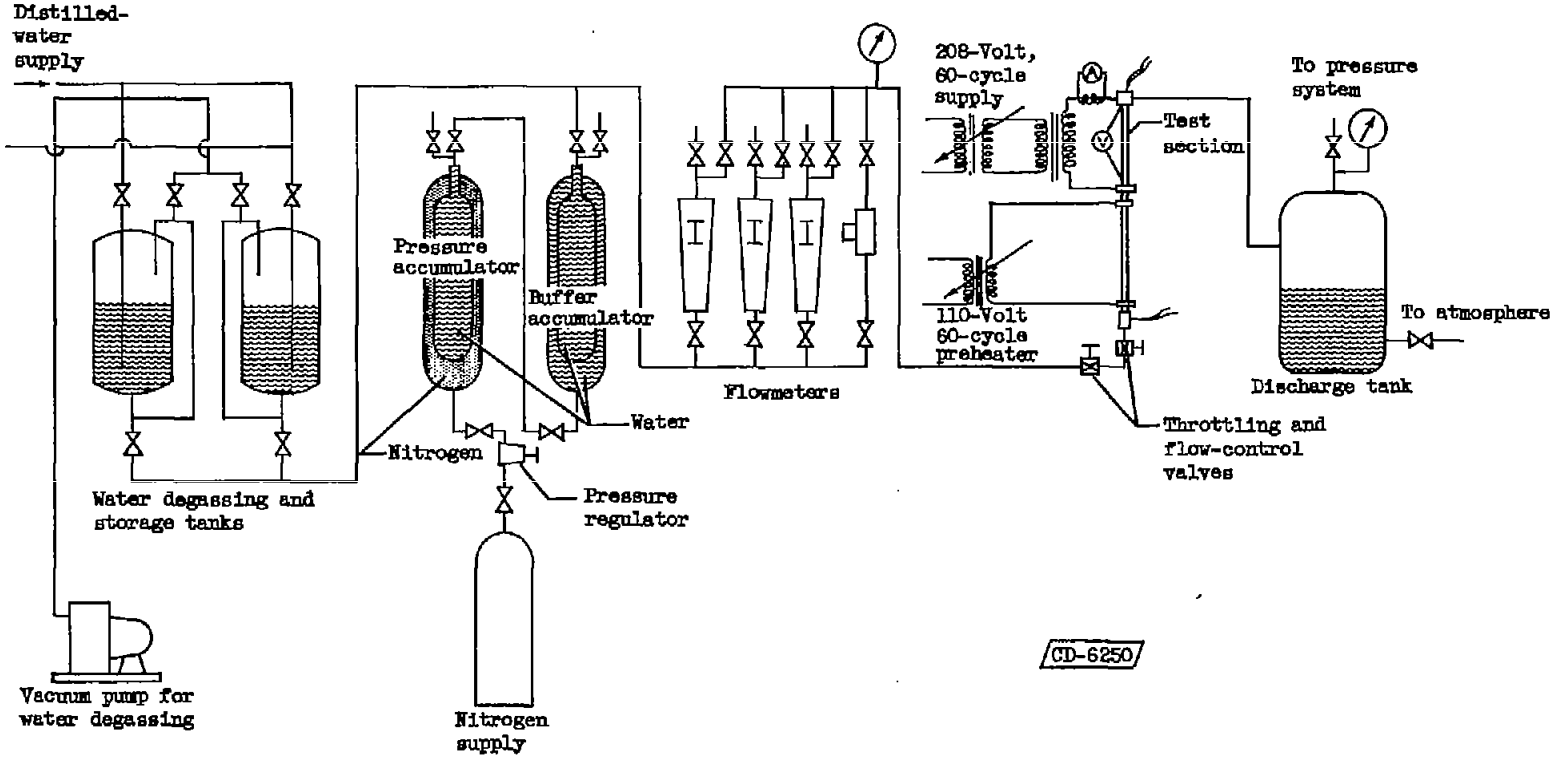

(b) Final.

Figure 1. - Concluded. Arrangement of apparatus.

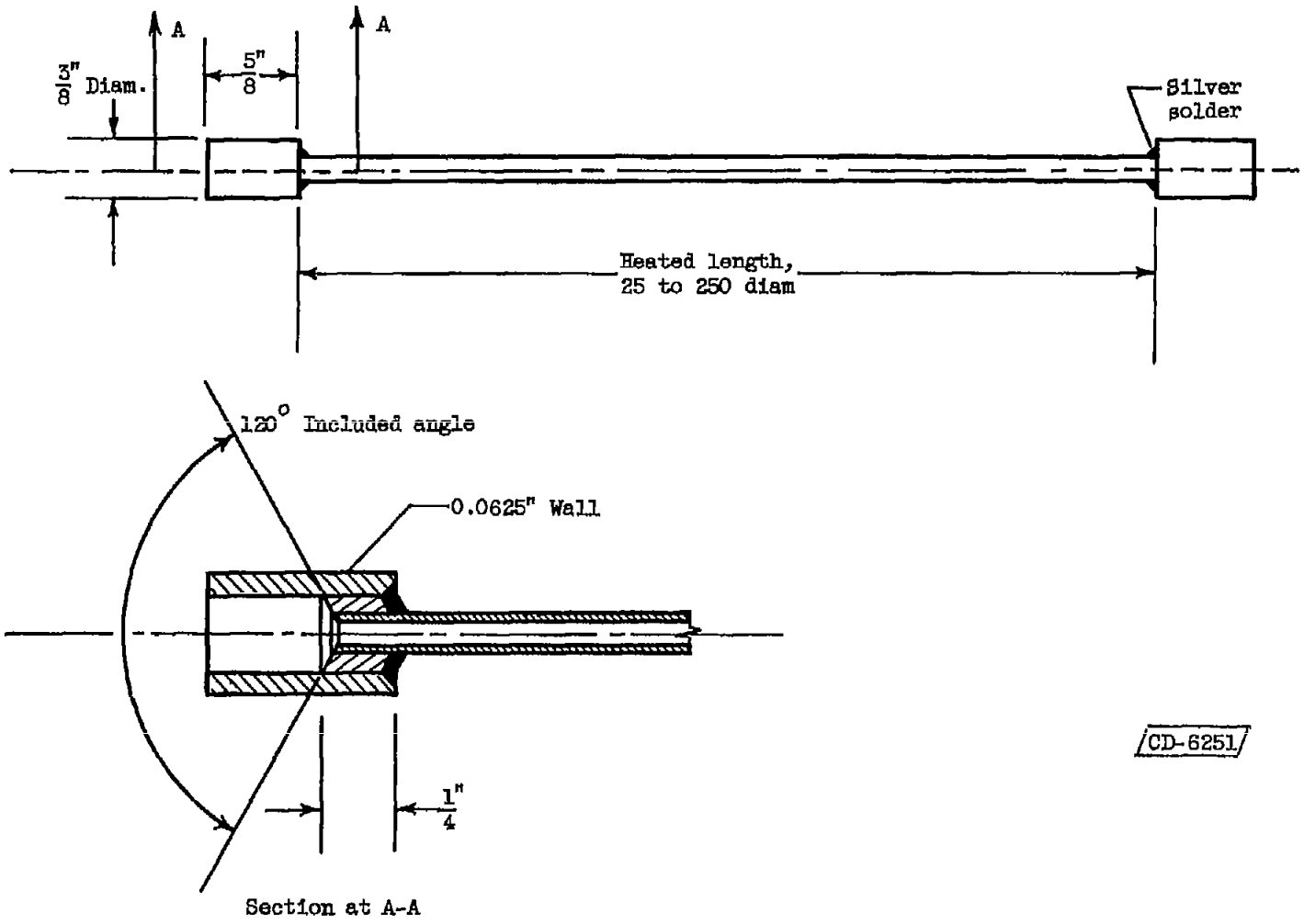

(a) Typical test section.

Figure 2. - Test section.

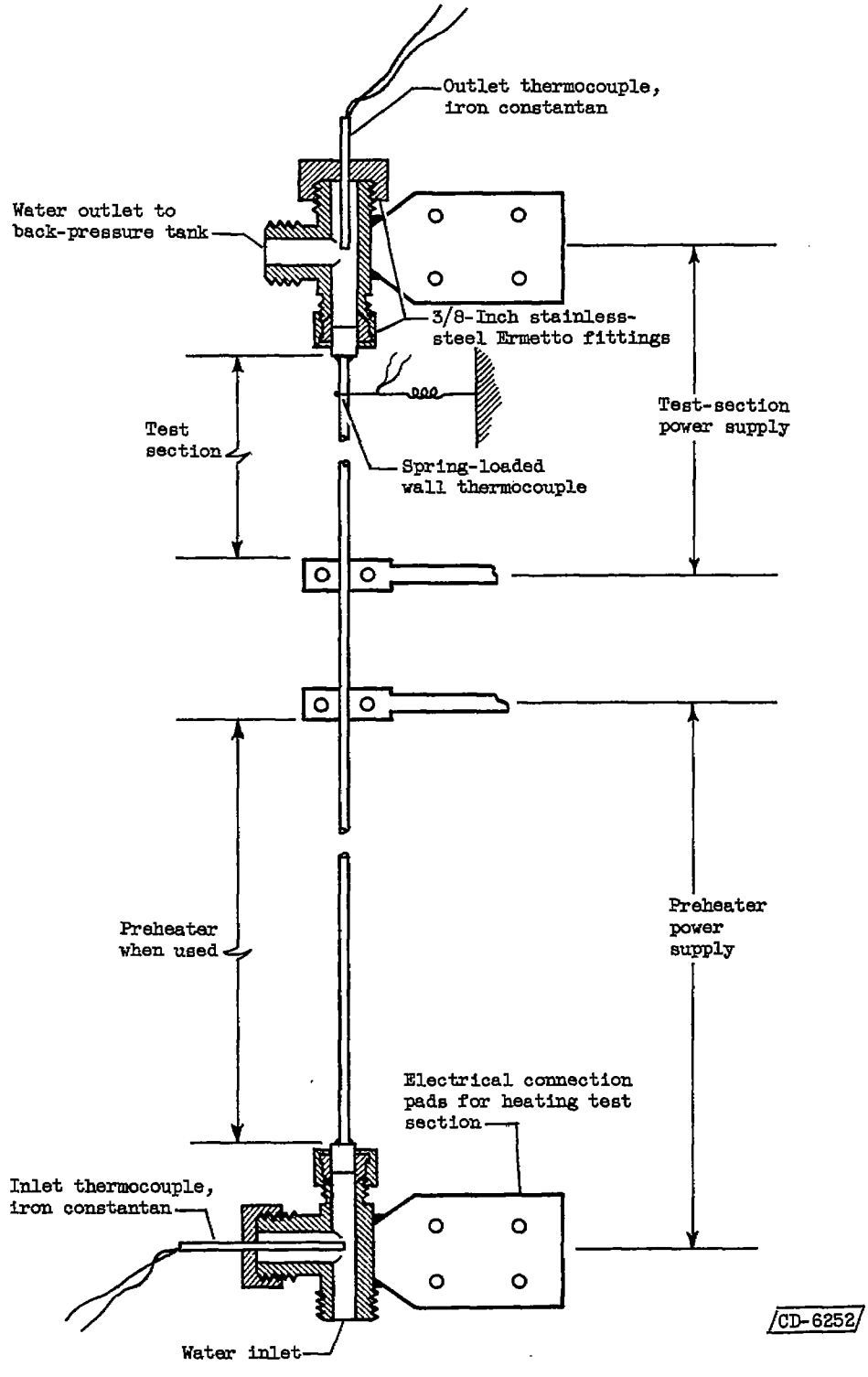

(b) Installation details.

Figure 2. - Concluded. Test section.

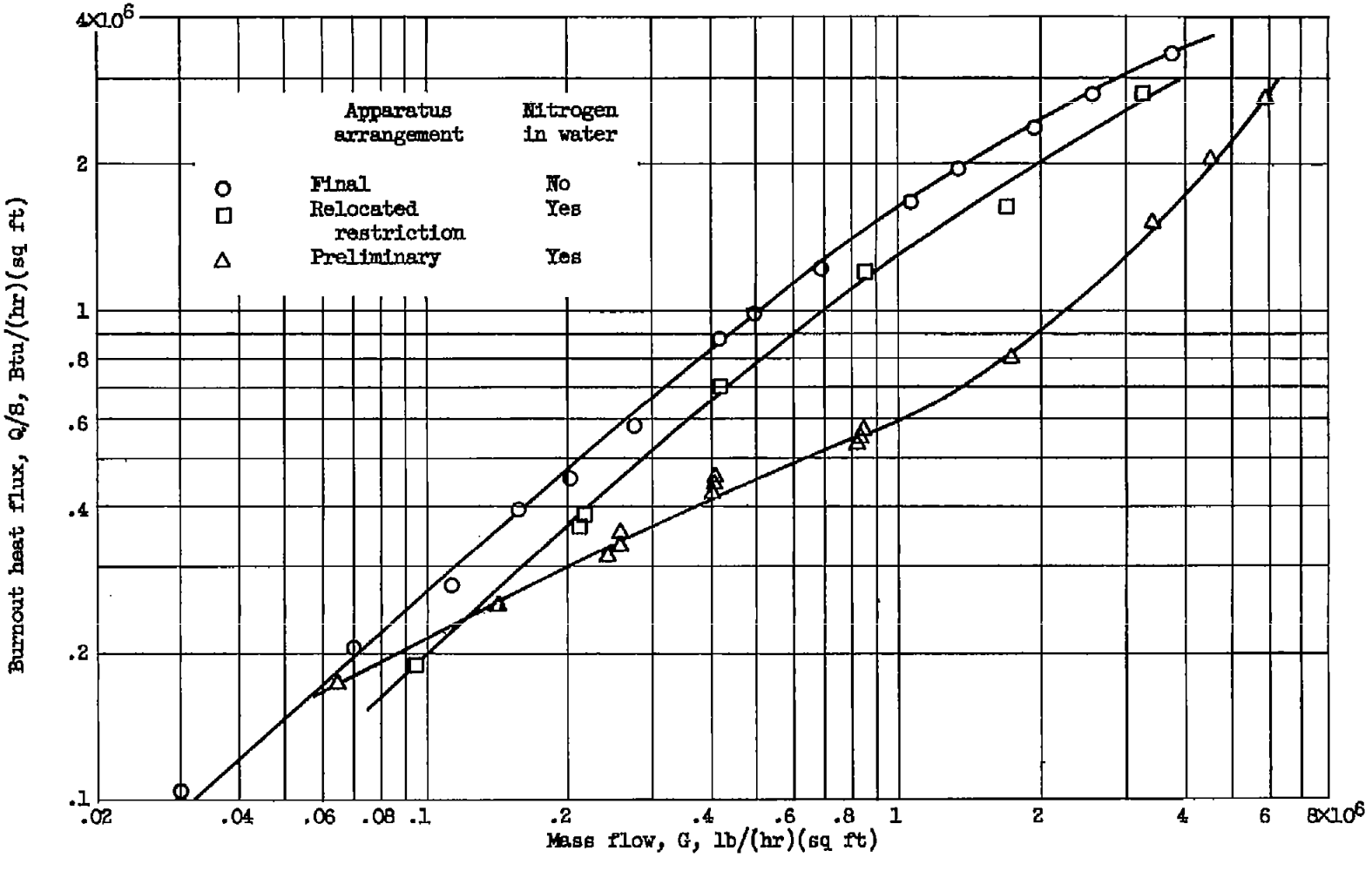

(a) Apparatus arrangement and nitrogen diffusion. Length-diameter ratio, 100; inside diameter, 0.123 inch; inlet temperature, 72° F; exit pressure, atmospheric; accumulator pressure, 300 pounds per square inch.

Figure 3. - Effect of apparatus arrangement on burnout.

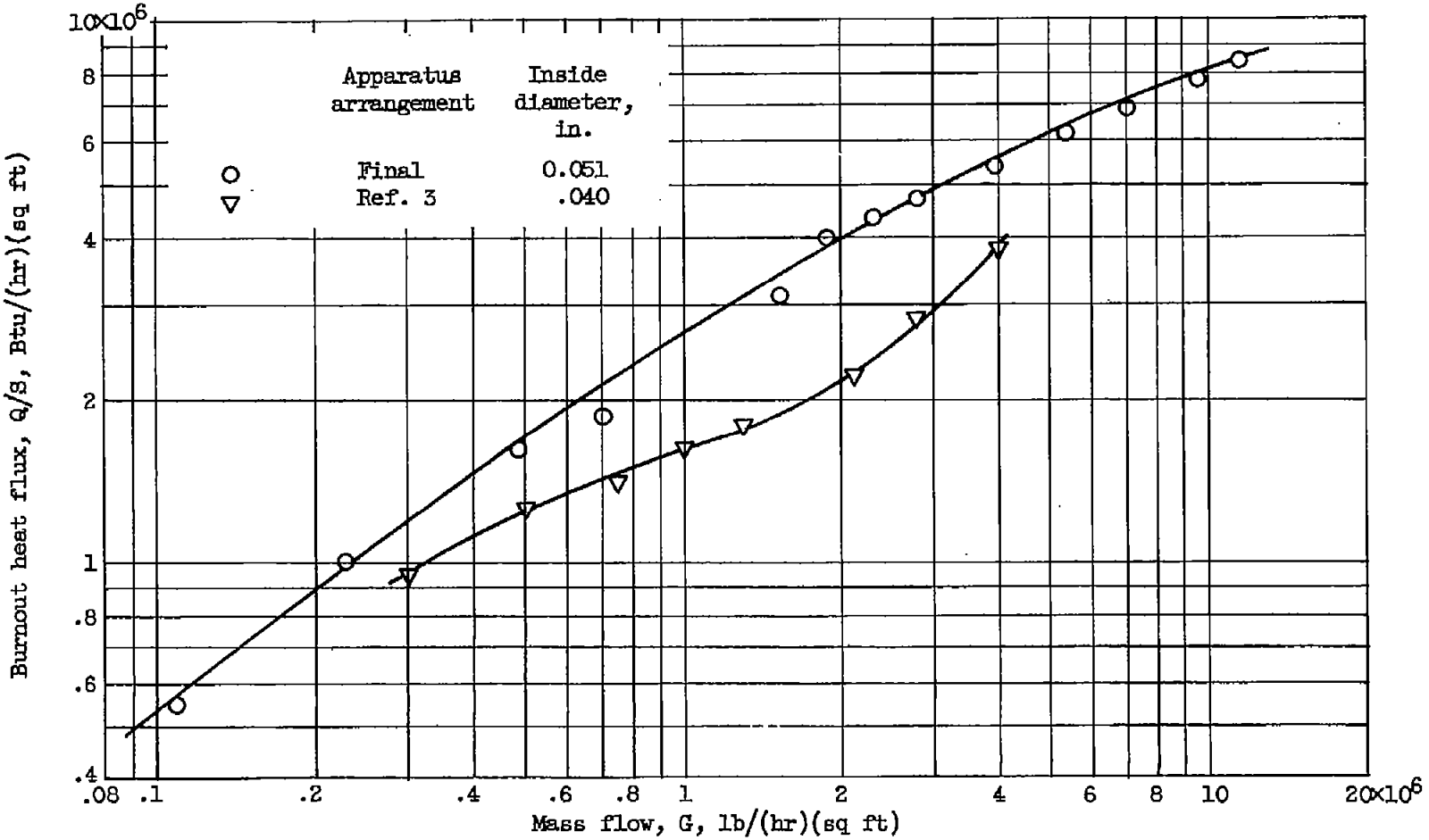

(b) Comparison of final arrangement with system of reference 3. Length-diameter ratio, 50; inlet temperature, 72° F; exit pressure, atmospheric.

Figure 3. - Concluded. Effect of apparatus arrangement on burnout.

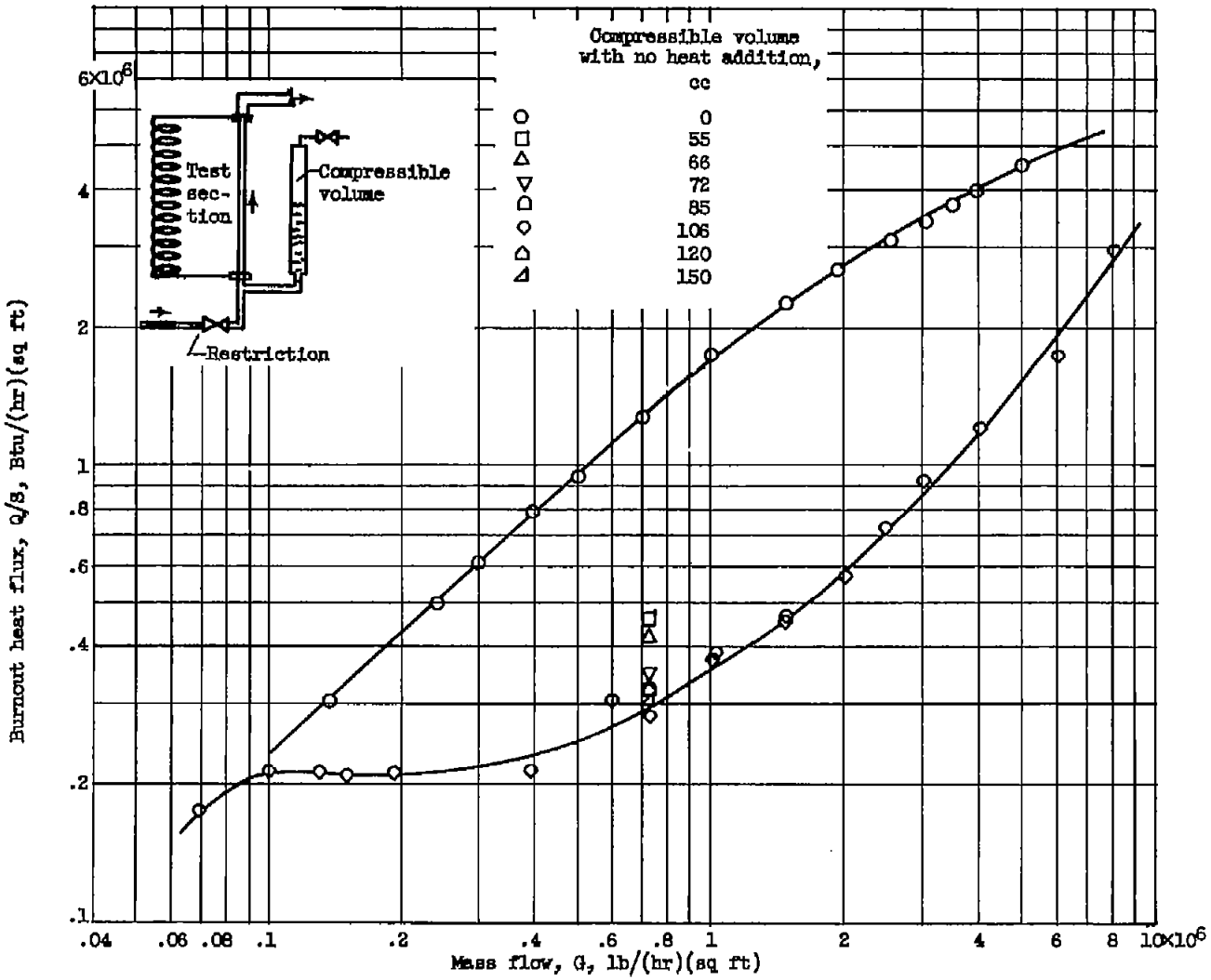

Figure 4. - Effect of compressible volume on burnout. Length-diameter ratio, 100; inside diameter, 0.096 inch; inlet temperature, 72° F; exit pressure, atmospheric; accumulator pressure, 300 pounds per square inch.

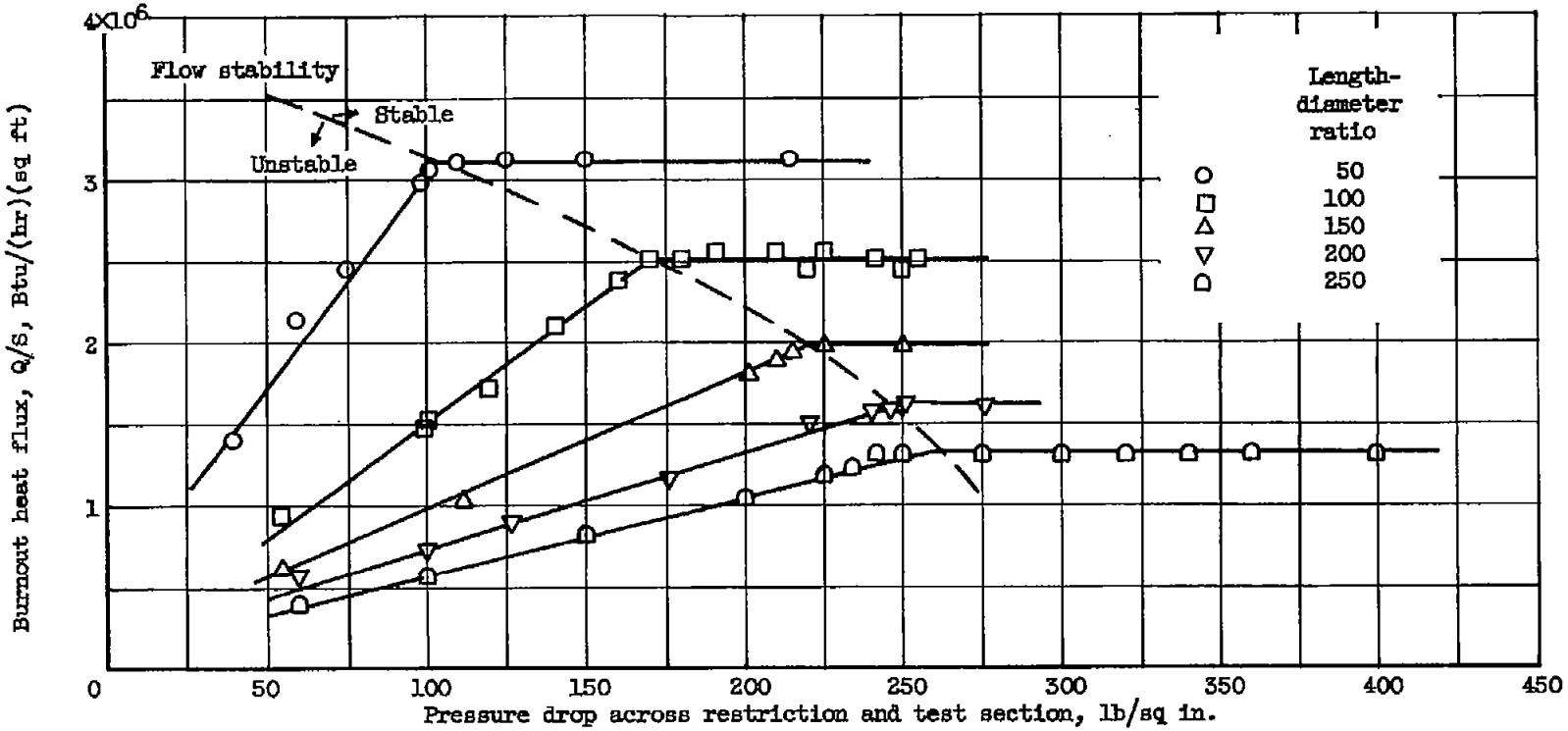

(a) Varying flow restriction for various test-section lengths. Mass-flow rate, 1.78×10^6 pounds per hour per square foot.

Figure 5. - Effect of flow restriction on flow stability and burnout. Tube diameter, 0.076 inch.

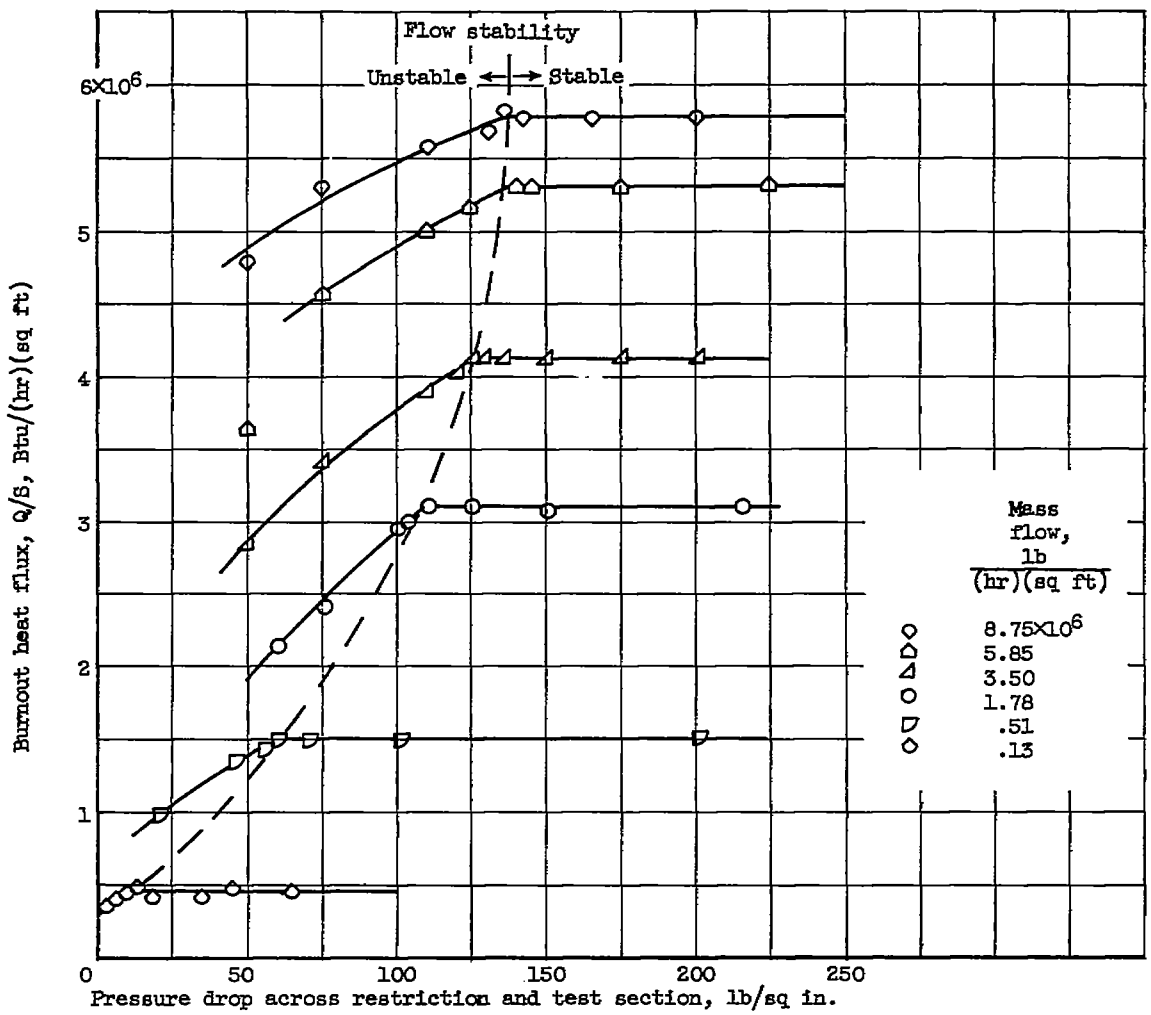

(b) Varying flow restriction for various mass-flow rates. Length-diameter ratio, 50.

Figure 5. - Concluded. Effect of flow restriction on flow stability and burnout. Tube diameter, 0.076 inch.

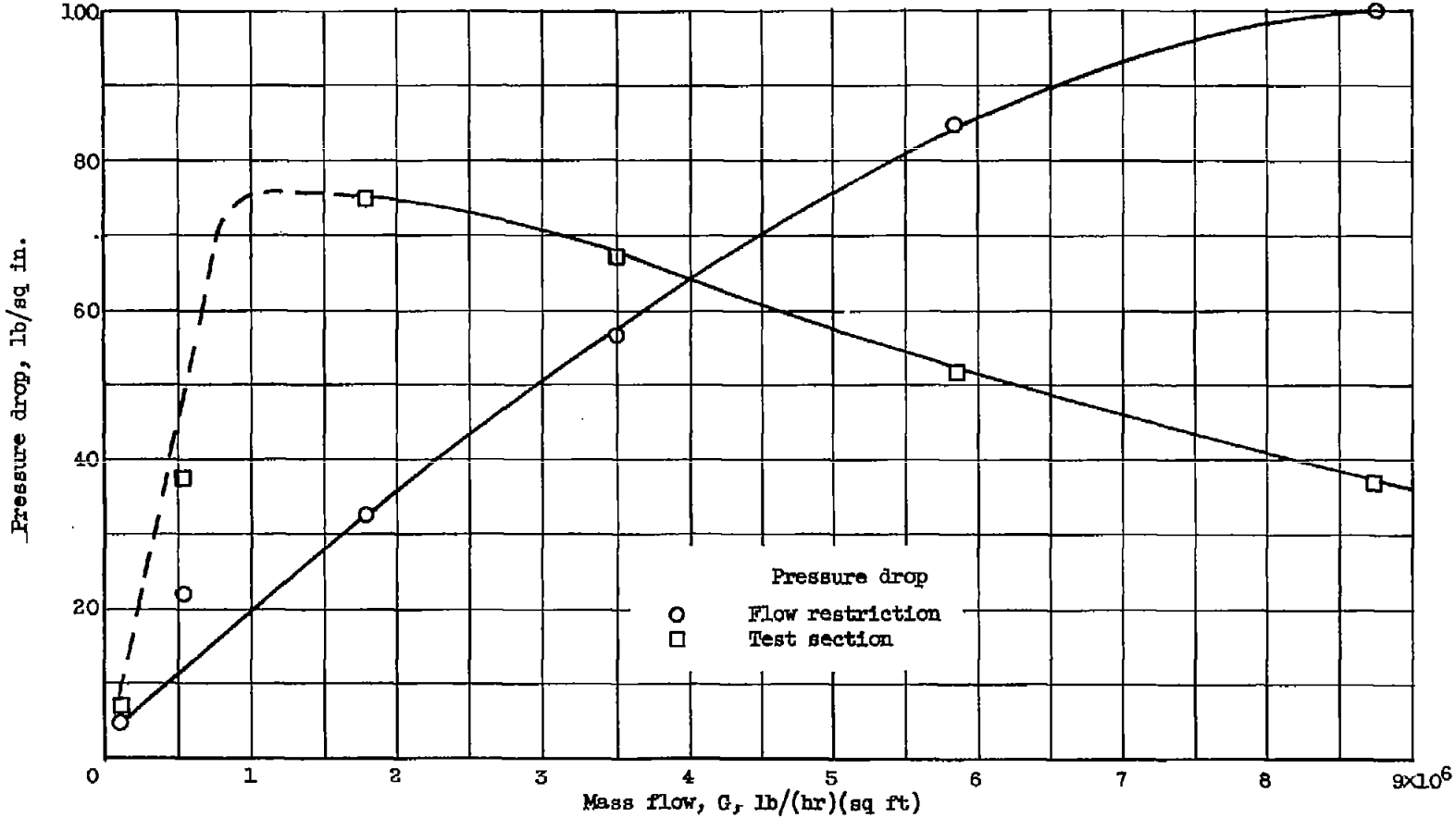

Figure 6. - Variation with flow rate of test-section pressure drop and minimum flow-restriction pressure drop required to stabilize flow.

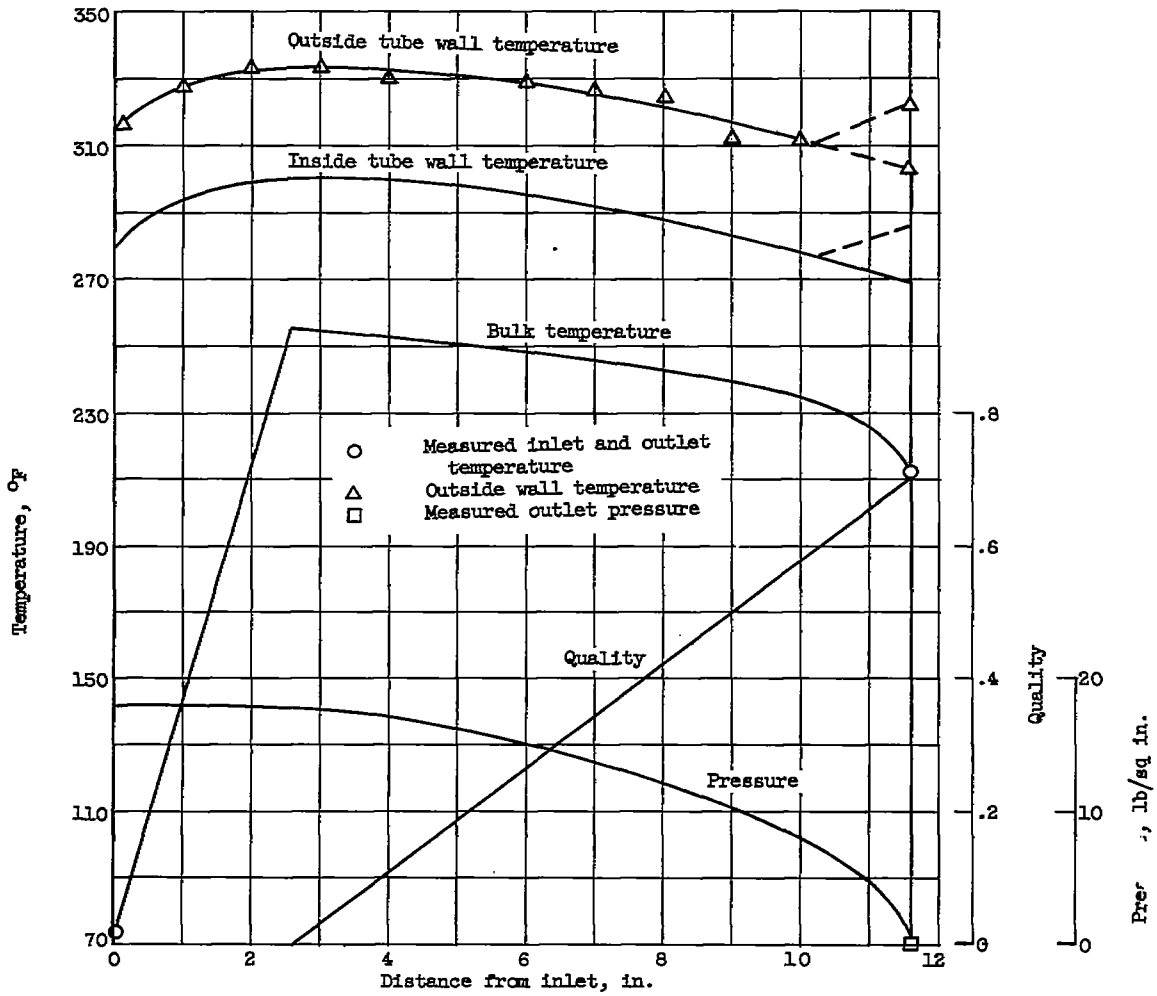

Figure 7. - Typical burnout conditions. Heat flux, 0.42×10^6 Btu per hour per square foot; mass flow, 0.21×10^6 pounds per hour per square foot; inside diameter, 0.116 inch; length, 11.6 inches; wall thickness, 0.020 inch.

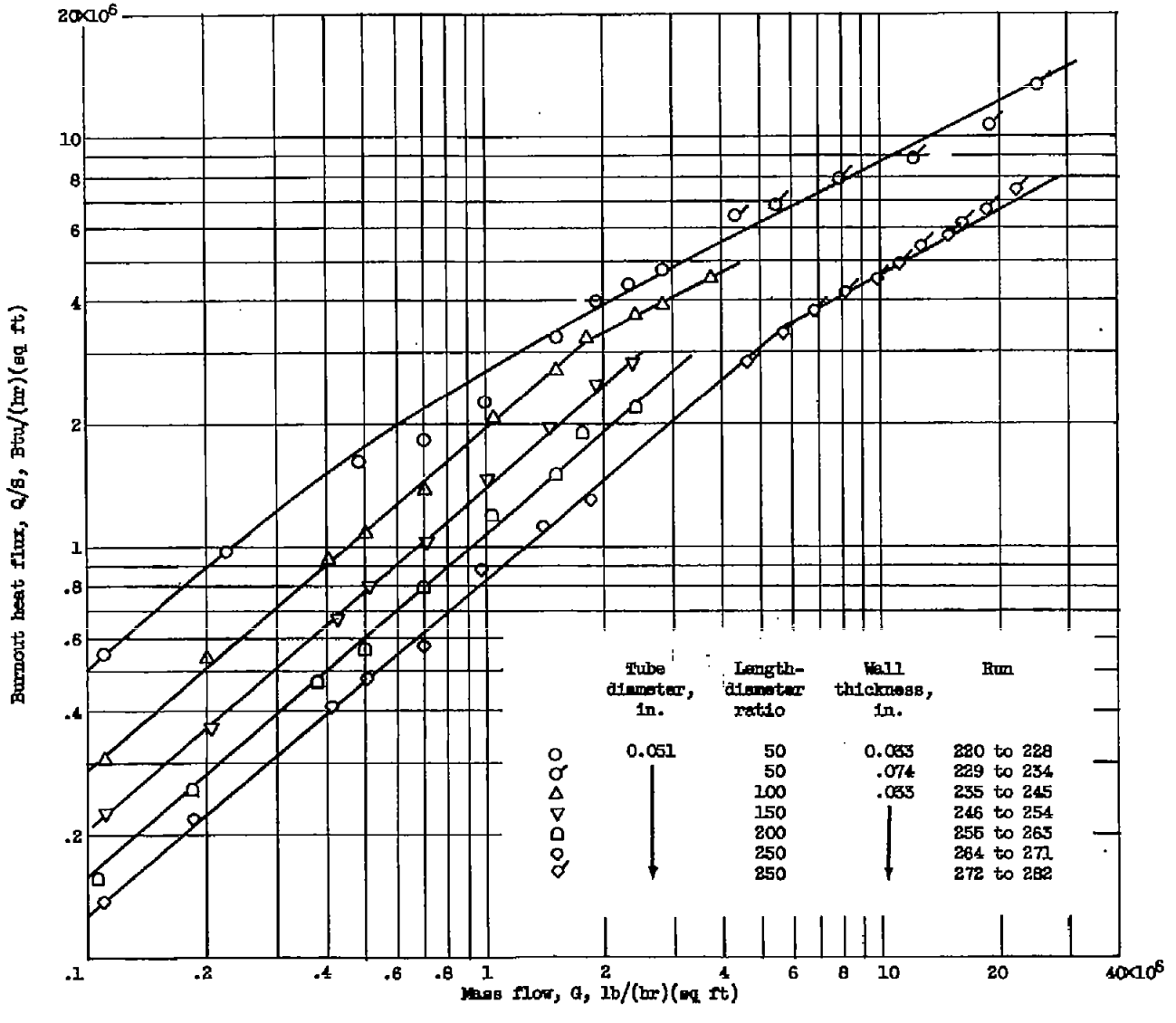

Figure 8. - Representative variation of burnout heat flux with mass flow and length-to-diameter ratio.

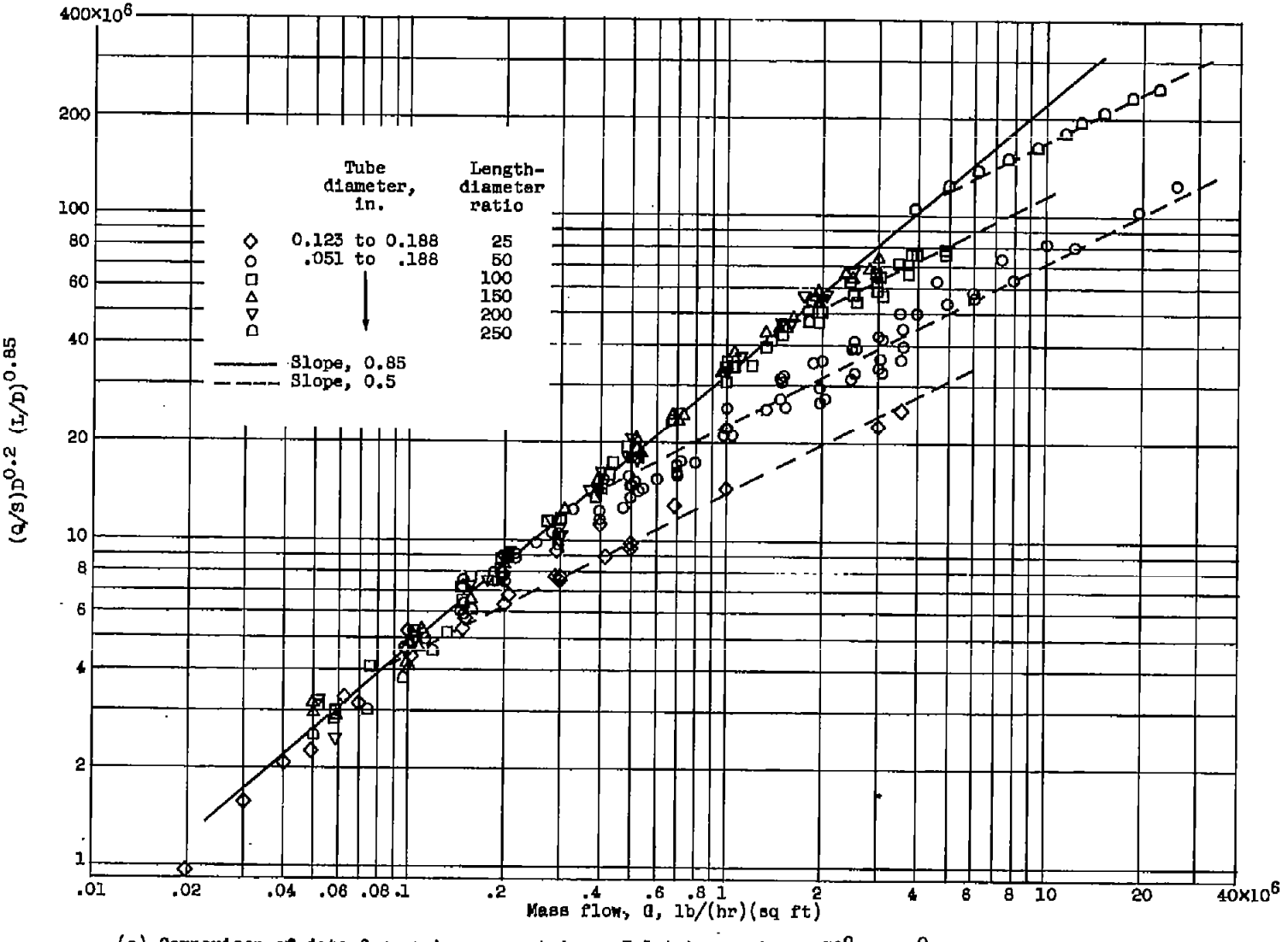

(a) Comparison of data for various geometries. Inlet temperature, 72° to 78° F; exit pressure, atmospheric.

Figure 9. - Effect of tube geometry on burnout.

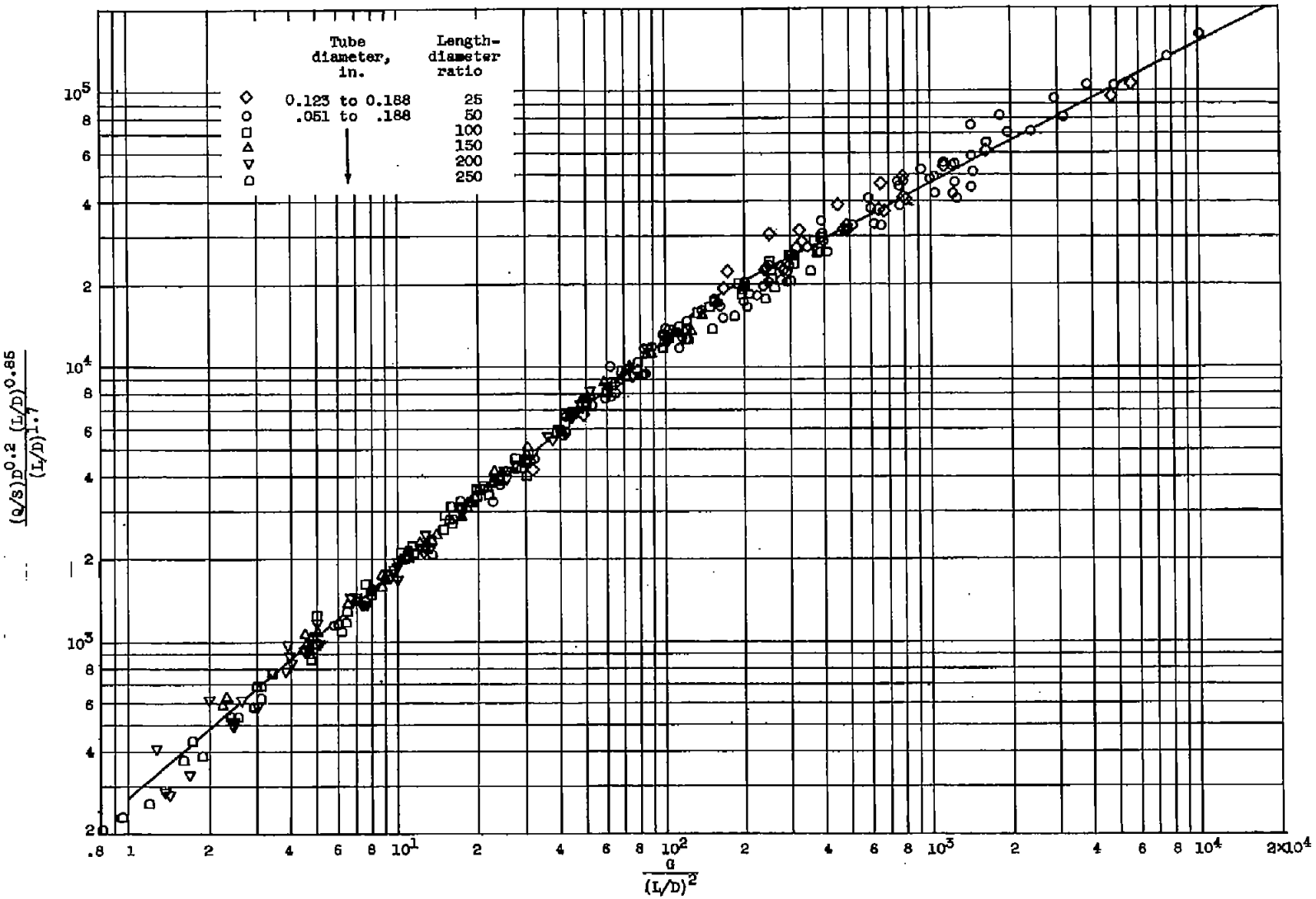

(b) Correlation of data.

Figure 9. - Continued. Effect of tube geometry on burnout.

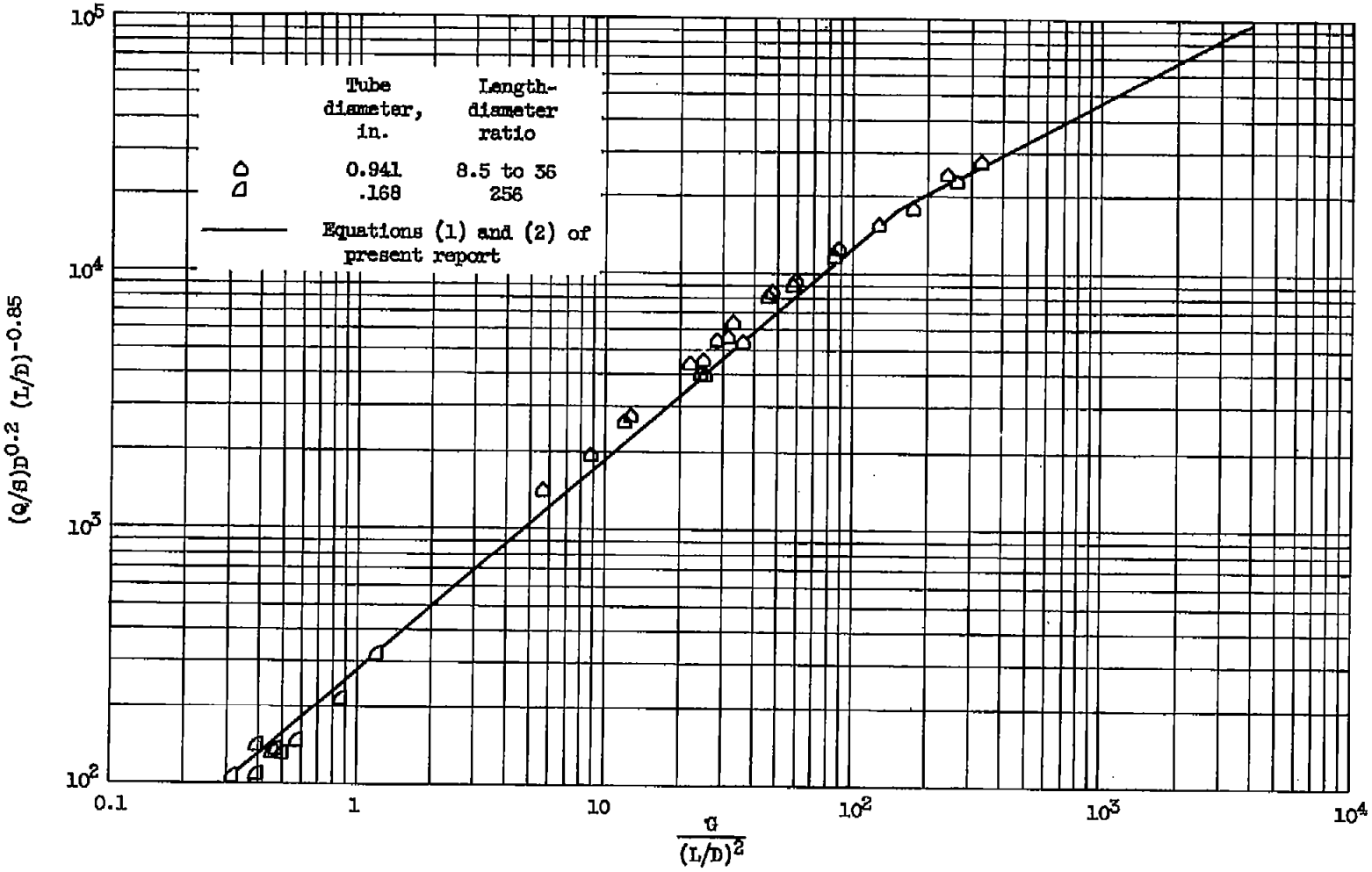

(c) Correlation of data from reference 4 and present report. Water inlet temperature, 70° F; exit pressure, atmospheric.

Figure 9. - Concluded. Effect of tube geometry on burnout.

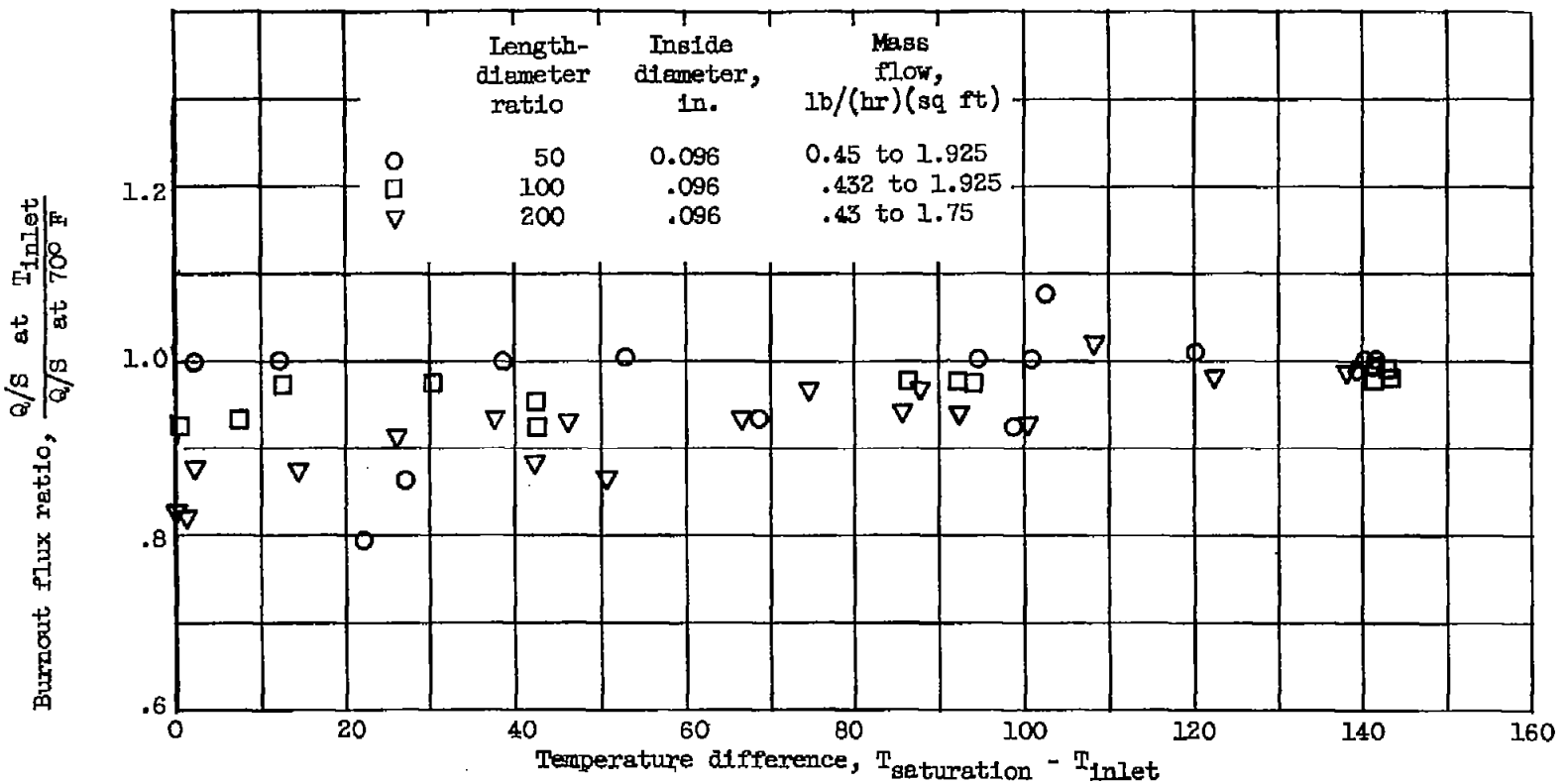

Figure 10. - Effect of variation of inlet temperature on burnout.

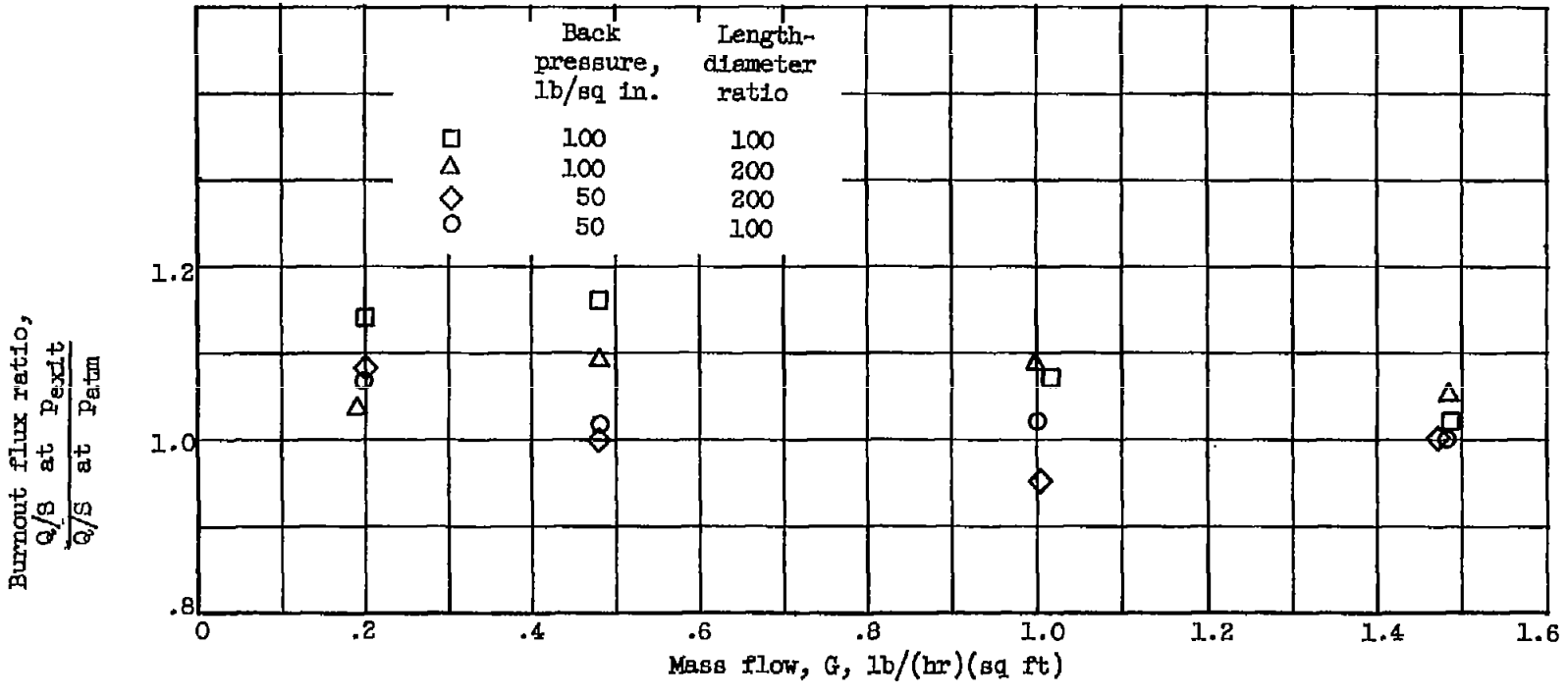

Figure 11. - Effect of variation of exit pressure on burnout. Inlet temperature, 72° F.